

Chunk Twice, Embed Once: A Systematic Study of Segmentation and Representation Trade-offs in Chemistry-Aware Retrieval-Augmented Generation

Mahmoud Amiri^{a,b}, Thomas Bocklitz^{a,b}

June 24, 2025

^a Leibniz Institute of Photonic Technology, Member of Research Alliance “Leibniz Health Technologies”, Jena, 07745, Germany

^b Institute of Physical Chemistry, Friedrich Schiller University Jena, 07743, Germany

Abstract

Retrieval-Augmented Generation (RAG) systems are increasingly vital for navigating the ever-expanding body of scientific literature, particularly in high-stakes domains such as chemistry. Despite the promise of RAG, foundational design choices—such as how documents are segmented and represented—remain underexplored in domain-specific contexts. This study presents the first large-scale, systematic evaluation of chunking strategies and embedding models tailored to chemistry-focused RAG systems. We investigate 25 chunking configurations across five method families and evaluate 48 embedding models on three chemistry-specific benchmarks, including the newly introduced *FSUChemRxivQuest* dataset. Our results reveal that recursive token-based chunking (specifically R100-0) consistently outperforms other approaches, offering strong performance with minimal resource overhead. We also find that retrieval-optimized embeddings—such as Nomic, and Intfloat E5 variants—substantially outperform domain-specialized models like SciBERT. By releasing our datasets, evaluation framework, and empirical benchmarks, we provide actionable guidelines for building effective and efficient chemistry-aware RAG systems.

Keywords: Retrieval-Augmented Generation, Chemistry NLP, Chunking strategies, Embedding models, Domain-specific language models.

1 Introduction

In recent years, the pace of research in chemistry has accelerated significantly, with thousands of new articles, preprints, and patents published each year[1]. This exponential growth in

domain-specific knowledge has led to an increasing demand for tools that can efficiently retrieve and synthesize information from large corpora[2]. Retrieval-Augmented Generation¹[3] systems have emerged as promising solutions, combining information retrieval with language generation to produce grounded, contextually aware answers. In scientific domains like chemistry—where factual accuracy, technical specificity, and interpretability are essential[4]—RAG pipelines must be finely tuned to the structure and semantics of domain texts.

Despite growing interest in applying RAG systems to chemistry[5–8], two foundational components of their retrieval stage remain underexplored: *chunking strategies*[9] and *embedding model selection*[10]. Chunking—i.e., the method for segmenting documents into retrievable units—can greatly influence the system’s ability to surface relevant passages. At the same time, the choice of *text embedding models* determines how chemical knowledge, nomenclature, and relationships are represented in vector space. Surprisingly, most existing studies in scientific QA either use naïve fixed-size chunking or adopt off-the-shelf embedding models without systematically evaluating their impact in domain-specific settings.

Past research often optimizes *either* chunking *or* embeddings in isolation, without examining their combined effects[11, 12]. Moreover, many evaluations rely on general-purpose benchmarks (e.g., Natural Questions[13] or MS MARCO[14]), which lack the structural complexity and domain-specific terminology present in chemical literature. To date, no comprehensive study has jointly investigated how chunking method, chunk size, and overlap settings interact with different embedding models in the context of chemistry-specific retrieval tasks. As a result, best practices remain unclear for practitioners building retrieval systems in the chemical sciences.

In this paper, we present a two-stage empirical study that systematically investigates the impact of chunking strategies and embedding models on retrieval performance in chemistry-focused retrieval-augmented generation (RAG) systems. Our study is the first to comprehensively explore this design space for chemistry-specific applications, and our contributions are as follows.

First, we conduct an extensive evaluation of chunking strategies by comparing five different methods—ranging from simple baselines to semantic-aware approaches—across multiple chunk sizes and overlap configurations. All chunking variants are tested using the OpenAI `text-embedding-3-large` model. This stage enables us to identify the optimal chunking configuration tailored for chemistry-based retrieval tasks.

Next, using the best-performing chunking setup, we benchmark 48 embedding models, covering a diverse range of general-purpose, scientific, and chemistry-specialized embeddings. To ensure domain relevance and robustness, we carry out evaluations on three chemistry-focused retrieval datasets: *FSUChemRxivQuest* (introduced in this work), *ChemHotpotQARetrieval*[12, 15–17], and *ChemNQRetrieval*[13].

A central contribution of our work is the introduction of *FSUChemRxivQuest*, a novel, high-

¹RAG

quality, MTEB-compatible retrieval benchmark. This dataset is built from curated question-answer pairs[18] extracted from ChemRxiv preprints, providing a valuable resource for the community to evaluate chemistry-specific retrieval systems.

Finally, we perform a comprehensive evaluation of retrieval performance using standard information retrieval metrics such as Recall@k, Mean Reciprocal Rank (MRR), and normalized Discounted Cumulative Gain (nDCG)[19]. We also conduct rigorous statistical significance testing to compare model performance across tasks. Through this study, we provide actionable insights and establish strong empirical baselines for the development of chemistry-aware RAG systems.

Our findings demonstrate that chunking strategies can account for substantial variance in retrieval quality, especially when used in tandem with embeddings tuned for scientific or chemical text. By releasing our evaluation framework, preprocessed dataset, and MTEB task code, we hope to accelerate progress in scientific RAG, particularly in domains like chemistry where traditional NLP assumptions often fall short.

2 Experimental results

2.1 Chunking Strategy Evaluation

In the first stage of our study, we systematically evaluated the impact of different chunking strategies on retrieval performance in a chemistry-specific RAG pipeline. Our goal was to isolate the effects of chunk size, overlap, and segmentation method, using a fixed embedding model and retrieval backend. To ensure a fair comparison, we adopted the chunking implementations, evaluation protocols, and indexing setup proposed by [11]. To control for embedding variability, all document chunks and queries were encoded using the OpenAI text-embedding-3-large model.

We performed a comprehensive grid search over chunking strategies, chunk sizes, and overlap ratios, using the OpenAI `cl100k` tokenizer for all configurations. We evaluated five chunking strategies. These included: (1) *Fixed-Token-Chunker*[20], (2) *Recursive-Token-Chunker*[20], (3) *Cluster-Semantic-Chunker*[11], (4) *LLM-Semantic-Chunker*[11], and (5) *Kamradt-Modified-Chunker*[11, 21]. For the Fixed-Token-Chunker and Recursive-Token-Chunker, we tested multiple chunk sizes ranging from 64 to 512 tokens, and around 20% to 25% overlap. For a selected chunk size (i.e., 100 tokens), we then varied the overlap ratio across five values: 0%, 20%, 40%, 60%, and 80%. This produced multiple overlap configurations for each base size. Kamradt-Modified-Chunker method was evaluated at discrete chunk sizes (i.e., 50, 100, 200, 400 tokens) without overlap variation. Semantic chunkers (Cluster-Semantic-Chunker and LLM-Semantic-Chunker) were evaluated as standalone strategies without size or overlap variation. In total, the grid comprised 25 unique configurations, each evaluated independently for downstream performance.

2.2 Embedding Models Evaluation

In the second stage of our study, we systematically evaluate the retrieval performance of a broad set of embedding models across multiple chemistry-focused benchmarks. The goal of this stage is to understand how different model architectures, training paradigms, and levels of domain specialization affect performance in information retrieval tasks tailored to the chemical sciences. This stage builds upon the chunking configuration identified in Stage 1, where Recursive-Token-Chunker with a 100-token window and without overlap was found to be optimal.

We selected a diverse collection of 48 embedding models from the Hugging Face model hub. These models span a range of design dimensions including general-purpose language models, multilingual encoders, and domain-specific models trained on scientific or chemical corpora.

To ensure strict reproducibility, each model was loaded with a fixed Git commit hash corresponding to its checkpoint at the time of experimentation. Embeddings were generated by mean pooling the final hidden layer of each model, unless otherwise specified in the model documentation. All input texts were truncated to a maximum length of 512 tokens to conform with typical input constraints of transformer-based encoders.

We introduce FSUChemRxivQuest, a specialized benchmark within the Massive Text Embedding Benchmark²[17] framework for evaluating dense retrieval systems in chemistry. Derived from ChemRxivQuest[18], this dataset repurposes question-answer pairs from ChemRxiv³, a chemistry preprint repository, into retrieval-oriented queries.

To comprehensively evaluate model performance, we selected three chemistry-specific retrieval benchmarks that capture a diverse set of information needs: FSUChemRxivQuest, ChemHotpotQARetrieval, and ChemNQRetrieval. Together, these three benchmarks test the retrieval models encompasses a wide range of subfields within chemistry, including general chemistry, organic chemistry, inorganic chemistry, physical chemistry, analytical chemistry, biochemistry, and environmental chemistry, offering a comprehensive view of their retrieval effectiveness.

2.3 Chunking-Level Retrieval Performance

The complete set of chunking configurations evaluated during our grid search is summarised in Table 1. For brevity, we reference each configuration by its corresponding *short name*, as listed in the final column of Table 1, throughout the remainder of this section.

A detailed breakdown of evaluation metrics—including IoU, Recall, Precision, and the domain-specific Precision Ω —is provided in Table 7 (section 7 Supplementary Material). These results span all 15 chunking strategies and offer a basis for comparative analysis. Figure 1 visualises metric distributions across corpora, enabling an assessment of performance variabil-

²MTEB

³<https://chemrxiv.org/>

Table 1: Overview of chunking strategies evaluated in this study. Each method is categorized by type, associated chunk size, and overlap size (if applicable). Short names are used throughout the paper for clarity and visual compactness in figures and tables.

Method	Chunk Size	Overlap Size	Short Name
Fixed-Token-Chunker	64	12	FX64-12
Fixed-Token-Chunker	128	25	FX128-25
Fixed-Token-Chunker	256	50	FX256-50
Fixed-Token-Chunker	512	100	FX512-100
Recursive-Token-Chunker	64	16	RT64-16
Recursive-Token-Chunker	100	20	RT100-20
Recursive-Token-Chunker	128	32	RT128-32
Recursive-Token-Chunker	256	64	RT256-64
Recursive-Token-Chunker	512	128	RT512-128
Kamradt-Modified-Chunker	50	–	KM50
Kamradt-Modified-Chunker	100	–	KM100
Kamradt-Modified-Chunker	200	–	KM200
Kamradt-Modified-Chunker	400	–	KM400
Cluster-Semantic-Chunker	–	–	CL
LLM-Semantic-Chunker	–	–	LLM

ity, while Figure 2 offers a complementary precision-recall perspective, aggregating results by chunking family for higher-level insight.

The results reveal a pronounced stratification across chunking strategies. Recursive-token methods consistently outperform other approaches. Notably, the RT64-16 configuration achieves the highest mean IoU (0.123 ± 0.093) and leads in Precision Ω (0.432 ± 0.147), while maintaining strong recall (0.638 ± 0.413). RT100-20 also performs competitively, offering a favourable balance between precision and recall, as indicated by its prominent position in the upper-right quadrant of the scatterplot in Figure 2a. The large F_1 -score bubbles associated with this configuration further highlight its strong trade-off characteristics.

In contrast, fixed-token methods perform well only at finer granularities. The strongest fixed variant, FX64-12, lags behind RT64-16 by approximately 33% in mean IoU and 15% in Precision Ω . Performance among fixed-token configurations degrades nearly monotonically with increasing token span, as observed from FX128-25 to FX512-100. This suggests that coarse chunking dilutes important domain-specific signals, likely due to the inclusion of extraneous or weakly relevant content.

Semantic chunkers such as CL and LLM display high recall values (averaging around 0.71) but suffer from substantially lower precision. Their IoU and Precision Ω scores are approximately half those of top recursive strategies, positioning them in the lower-left quadrant of Figure 2a. This implies a tendency to retrieve broadly relevant but weakly aligned content—a trade-off that may be unsuitable in high-precision domains.

Kamradt-modified chunkers fall in the middle of the performance spectrum. While their precision metrics are comparable to FX64-12, they trail recursive strategies in recall, resulting in moderate F_1 and F_2 scores and an overall average performance profile.

When aggregating performance by method family (Figure 2b), the recursive family maintains a clear lead with a mean IoU@10 of 0.068. Fixed-token methods follow at a 32% deficit,

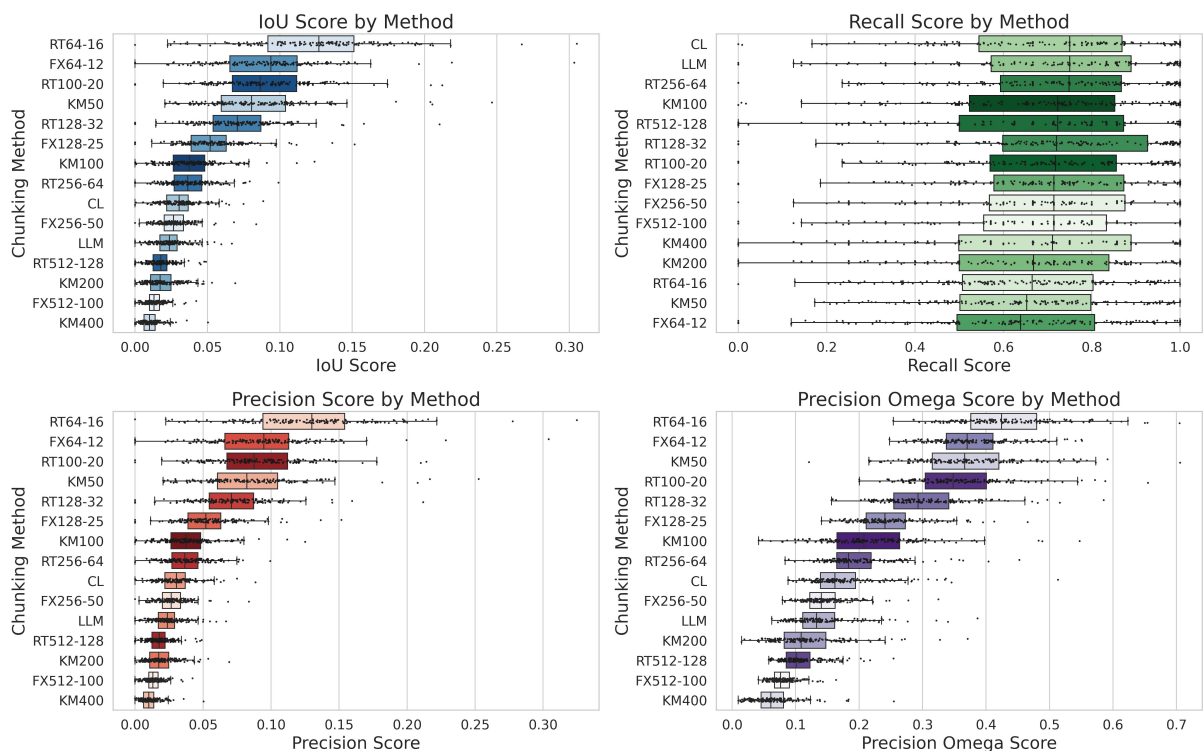
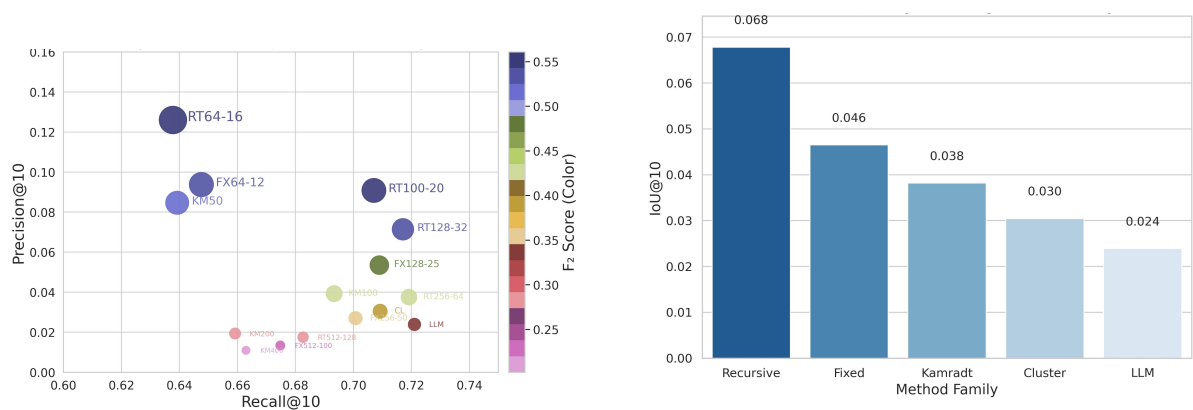


Figure 1: Corpus-level performance distributions for chunking strategies across four retrieval metrics. Boxplots (with overlaid jittered points) show score distributions across multiple chemistry corpora for each chunking method. Metrics include Intersection-over-Union (IoU), Recall, Precision, and Precision@ Ω . Recursive strategies (e.g., R64-16, RT100-20) consistently outperform others, with higher medians and lower variance, particularly for precision-oriented metrics.



(a) Precision vs. Recall by chunking method. Point size encodes F_1 score and color encodes F_2 score. Recursive strategies (e.g., R64-16, RT100-20) exhibit the best precision-recall balance.

(b) Mean IoU@10 by chunking method family. Recursive methods significantly outperform others, underscoring the efficacy of hierarchical, token-based chunking.

Figure 2: Comparison of chunking strategy performance: (a) Precision-recall trade-offs with F_1 and F_2 scores represented by size and color, respectively; (b) Mean IoU@10 grouped by chunking family.

Kamradt-modified methods at 44%, cluster-based chunkers at 56%, and LLM-based methods at 65%. This trend underscores the advantage of recursive, token-aware segmentation, which adaptively determines chunk boundaries based on syntactic or structural cues, thereby preserving semantic coherence.

These findings show that recursive strategies yield not just marginal improvements, but substantial gains in retrieval performance. Their capacity to maintain fine-grained context without sacrificing alignment is particularly advantageous for tasks involving complex technical literature, such as chemical text retrieval.

Taken together, the results support the use of small, overlapping recursive chunks in downstream retrieval and embedding tasks. While both RT64-16 and RT100-20 demonstrate strong performance, RT100-20 achieves the highest F_2 score among all evaluated configurations, indicating superior performance under recall-weighted evaluation. As shown in Table 8 (section 7 Supplementary Material), RT100-20 also maintains one of the highest recall values, making it particularly well-suited for retrieval tasks where comprehensive content coverage is critical. Although RT64-16 offers slightly better precision and excels in metrics such as IoU and Precision Ω , its overall balance under recall-focused criteria is slightly outperformed by RT100-20. In contrast, large monolithic chunks—particularly those exceeding 256 tokens—consistently underperform. While they may offer reduced index size or query latency, these benefits come at the expense of retrieval fidelity and should only be considered in latency-sensitive scenarios.

Most importantly, our results demonstrate that chunking configuration has a critical impact on retrieval performance—comparable to, or greater than, the influence of the embedding model itself. The observed tenfold variation in IoU across chunking strategies highlights the necessity of rigorously reporting and optimising segmentation parameters in RAG system design, especially in high-stakes technical and scientific domains.

These findings establish a strong foundation for the analyses presented in Section 3, where we evaluate the impact of different embedding models within the optimal chunking framework identified here.

2.4 Overlap-Ratio Sensitivity (Fixed 100-Token Span)

To systematically assess the impact of **intra-chunk overlap** on retrieval performance, we evaluated ten configurations using a fixed chunk length of 100 tokens (Table 2). For clarity, we use the shorthand names throughout this section.

Complete evaluation results, including per-metric and per-corpus statistics, are provided in Table 9 (section 7 Supplementary Material). Figure 3 visualizes the corpus-level distribution of performance metrics, while Figure 4 captures trade-offs between precision and recall and highlights aggregated trends by chunking family.

Table 2: Overview of chunking strategies evaluated in this overlap analysis. All methods share a consistent chunk size of 100 tokens, with varying overlap values ranging from 0 to 80. Fixed and recursive token chunkers are listed with their respective short identifiers used throughout the study.

Method	Chunk Size	Overlap Size	Short Name
Fixed-Token-Chunker	100	0	FX100-0
Fixed-Token-Chunker	100	20	FX100-20
Fixed-Token-Chunker	100	40	FX100-40
Fixed-Token-Chunker	100	60	FX100-60
Fixed-Token-Chunker	100	80	FX100-80
Recursive-Token-Chunker	100	0	RT100-0
Recursive-Token-Chunker	100	20	RT100-20
Recursive-Token-Chunker	100	40	RT100-40
Recursive-Token-Chunker	100	60	RT100-60
Recursive-Token-Chunker	100	80	RT100-80

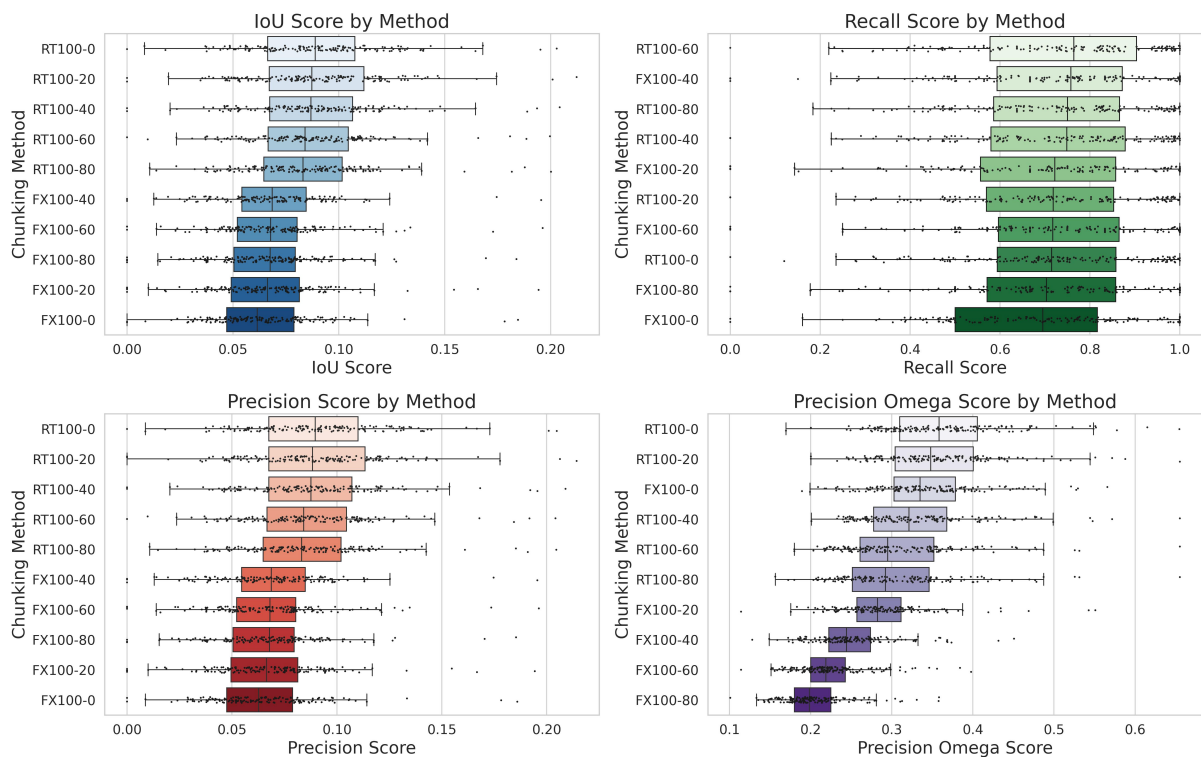
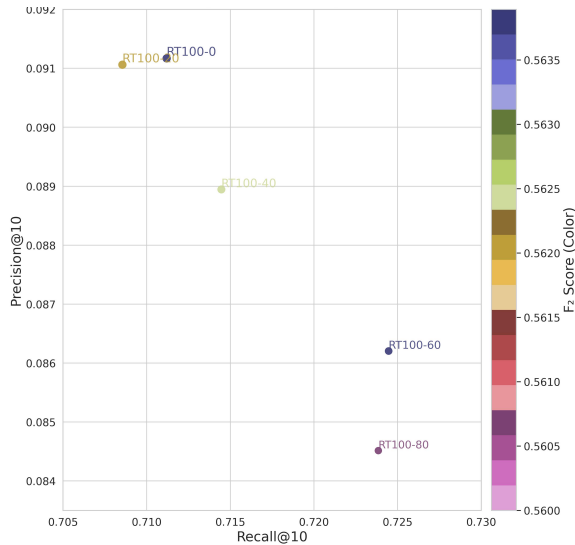
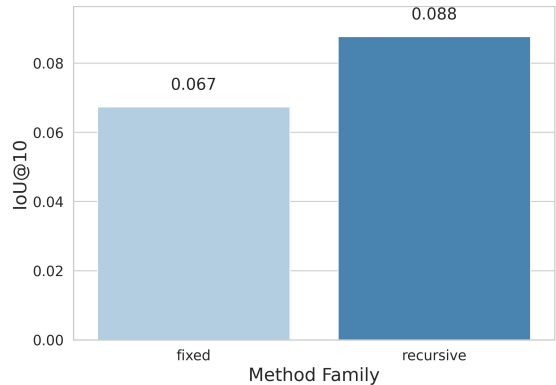


Figure 3: Corpus-level retrieval metric distributions across chunking methods. Subplots show IoU Score, Recall@10, Precision@10, and Precision Ω @10. Boxplots reflect metric spread across corpora; overlaid strip plots show individual data points. Recursive methods generally yield higher and more consistent scores.



(a) Precision vs. Recall. Color encodes F_2 .



(b) Mean IoU@10 grouped by chunking method family.

Figure 4: Comparative analysis of retrieval performance. (a) Trade-offs between recall and precision. (b) Family-aggregated IoU@10 scores. Recursive methods outperform across metrics.

Recursive chunking consistently outperforms fixed-span chunking across all metrics and corpora. The best-performing recursive configuration, RT100-0 (no overlap), achieves an IoU of 0.090 ± 0.067 , surpassing the best fixed-span variant, FX100-40 (0.069 ± 0.049), by approximately 30%. For domain-weighted precision, the margin is even greater: RT100-0 yields a $\text{Precision}\Omega$ of 0.365 ± 0.149 , a 45% improvement over FX100-40 (0.251 ± 0.078).

The influence of overlap ratio is nuanced and varies between chunking families. As shown in Table 10, fixed-span chunking experiences a short-lived boost in recall with moderate overlap (40–60 tokens), peaking at 0.727. However, this comes at the cost of a significant decline in precision. Beyond 20% overlap, $\text{Precision}\Omega$ drops by over 40%, leading to overall reductions in both F_1 and F_2 scores. Thus, although recall improves, the loss in specificity outweighs the benefits.

In contrast, recursive chunking displays more balanced trade-offs. Recall rises modestly from 0.711 at 0% overlap to 0.724 at 60%, but this gain is accompanied by a proportionally larger drop in precision. This asymmetry leads to diminishing returns. As illustrated in Figure 4a, only RT100-0 and RT100-60 offer meaningful precision–recall trade-offs, contingent on whether index efficiency or recall takes priority.

Aggregated results in Figure 4b further underscore the advantage of recursive segmentation. With a mean IoU of 0.088, recursive methods outperform fixed-span chunking (0.067) by 31%. This performance gap remains consistent regardless of overlap, reinforcing the benefits of token-aware, hierarchical segmentation over uniform slicing strategies.

Based on these findings, several actionable insights emerge for practitioners deploying retrieval-augmented systems in scientific domains. First, non-overlapping recursive chunking (RT100-0) is the most effective default strategy, offering a strong balance between perfor-

mance and efficiency, with F_1 and F_2 scores of 0.162 and 0.564, respectively, and requiring minimal index size.

Second, overlap should be introduced selectively, particularly in scenarios where recall is paramount. For example, RT_{100-60} increases recall to 0.725, but incurs a 60% increase in index size and a 15% drop in Precision Ω . These trade-offs are acceptable only when justified by the task requirements, such as in exploratory search or systematic reviews.

Lastly, high-overlap fixed-span chunking is discouraged. Overlap beyond 20% results in steep precision losses—with little to no gain in recall—making it unsuitable for precision-sensitive use cases.

Taken together with findings from Section 2.3, these results establish RT_{100-0} as the most robust and performant segmentation baseline for downstream embedding model evaluation and deployment in retrieval-heavy scientific applications.

3 Embedding–Model Evaluation

With the chunking strategy fixed to the optimal segmentation recipe (RT_{100-0} ; see Section 2.4), we evaluated a comprehensive suite of 48 open-source embedding models for chemistry-focused retrieval. These evaluations were conducted across three distinct benchmarks—*ChemHotpotQARetrieval*, *ChemNQRetrieval*, and the newly introduced *FSUChemRxivQuest*—each designed to capture different retrieval scenarios ranging from highly structured question-answer pairs to noisy, heterogeneous pre-publication scientific texts. Table 3 presents the full list of evaluated models, with abbreviated names used throughout the remainder of the paper for clarity and brevity.

Table 3: Decomposed Model Identifiers and Their Abbreviated Short Names. This table lists the full Hugging Face model identifiers along with their corresponding libraries, size or architecture details, version numbers (if applicable), and standardized short names used throughout the paper. These short names are referenced in various sections to simplify model comparison and discussion.

Library	Model	Size/Layer	Version	Short Name
sentence-transformers	all-MiniLM	L6	v2	Sent_MiniLM6_v2[22, 23]
sentence-transformers	all-MiniLM	L12	v2	Sent_MiniLM12_v2[23, 24]
sentence-transformers	all-mpnet-base	–	v2	Sent_allMPNetB_v2[23, 25]
sentence-transformers	gtr-t5	base	–	Sent_gtrT5_B[23, 26]
sentence-transformers	gtr-t5	large	–	Sent_gtrT5_L[23, 27]
sentence-transformers	gtr-t5	xl	–	Sent_gtrT5_XL[23, 28]
sentence-transformers	bert-base-nli-mean-tokens	–	–	Sent_BERTnli[23, 29]
sentence-transformers	multi-qa-mpnet-base-dot	v1	–	Sent_MQA_MPNetB[23, 30]
sentence-transformers	paraphrase-multilingual-MiniLM	L12	v2	Sent_paraMiniLM12[23, 31]
sentence-transformers	paraphrase-multilingual-mpnet-base	–	v2	Sent_paraMPNetB_v2[23, 32]
microsoft	BiomedNLP-BiomedBERT-abstract-fulltext	–	–	MS_BiomedBERT_af[33, 34]
microsoft	BiomedNLP-BiomedBERT-abstract	–	–	MS_BiomedBERT_a[33, 35]
microsoft	BiomedNLP-PubMedBERT-abstract-fulltext	–	–	MS_PubMedBERT_af[33, 36]
microsoft	BiomedNLP-PubMedBERT-abstract	–	–	MS_PubMedBERT_a[33, 37]
microsoft	MiniLM	L12-H384	–	MS_MiniLM384[38, 39]

Continued on next page

Table 3 – continued from previous page

Library	Model	Size/Layer	Version	Short Name
microsoft	mpnet	base	–	MS_MPNetB[40, 41]
intfloat	e5	small	v1	Intf_e5S[42, 43]
intfloat	e5	small	v2	Intf_e5S_v2[42, 44]
intfloat	e5	base	v1	Intf_e5B[42, 45]
intfloat	e5	base	v2	Intf_e5B_v2[42, 46]
intfloat	e5	large	v1	Intf_e5L[42, 47]
intfloat	e5	large	v2	Intf_e5L_v2[42, 48]
intfloat	multilingual-e5	base	–	Intf_mE5B[42, 49]
intfloat	multilingual-e5	large	–	Intf_mE5L[42, 50]
intfloat	multilingual-e5	small	–	Intf_mE5S[42, 51]
BAAI	bge	small-en	–	BAAI_bgeS[52, 53]
BAAI	bge	small-en	v1.5	BAAI_bgeS_v1.5[52, 54]
BAAI	bge	base-en	–	BAAI_bgeB[52, 55]
BAAI	bge	base-en	v1.5	BAAI_bgeB_v1.5[52, 56]
BAAI	bge	large-en	–	BAAI_bgeL[52, 57]
BAAI	bge	large-en	v1.5	BAAI_bgeL_v1.5[52, 58]
BAAI	bge	m3	–	BAAI_bgeM3[59, 60]
nomic-ai	nomic-embed-text	–	v1	Nomic_text_v1[61, 62]
nomic-ai	nomic-embed-text	–	v1.5	Nomic_text_v1.5[62, 63]
nomic-ai	nomic-bert	2048	–	Nomic_BERT2048[64, 65]
facebook	contriever	–	–	FB_contriever[66, 67]
facebook	contriever-msmarco	–	–	FB_contrieverMS[66, 68]
DeepChem	ChemBERTa	77M	MTR	DC_ChemBERTa[69, 70]
google	bert-base-uncased	base	–	GGL_BERTbU[71]
jinaai	jina-embeddings-v2	base-en	v2	Jina_v2B[72, 73]
jinaai	jina-embeddings-v2	small-en	v2	Jina_v2S[73, 74]
m3rg-iitd	matscibert	–	–	IITD_MatSci[75, 76]
describeai	gemini	–	–	Desc_Gemini[77]
hkunlp	instructor-xl	xl	–	HKU_InstructXL[78, 79]
allenai	scibert-scivocab-uncased	base	–	AI_SciBERT[80, 81]
allenai	specter	–	–	AI_Specter[82, 83]
recobo	chemical-bert-uncased	–	–	Rec_ChemBERT[84]
sentence-transformers	paraphrase-multilingual-mpnet-base	–	v2	Sent_paraMPNetB_v2[23, 85]

All models were assessed under the MTEB protocol using six standard retrieval metrics: Main Score, NDCG@10, MAP@10, Recall@10, Precision@10, and MRR@10. This evaluation framework ensured comparability across models and decoupled model performance from infrastructural artifacts. Figure 5 summarizes the top-15 models across all tasks and metrics, showing that retrieval-tuned models such as `Nomic_text_v1.5`, `BAAI_bgeL_v1.5`, `Intf_mE5L`, `Intf_e5B`, and `Intfloat_e5L_v2` consistently dominate performance across both precision- and recall-oriented evaluations.

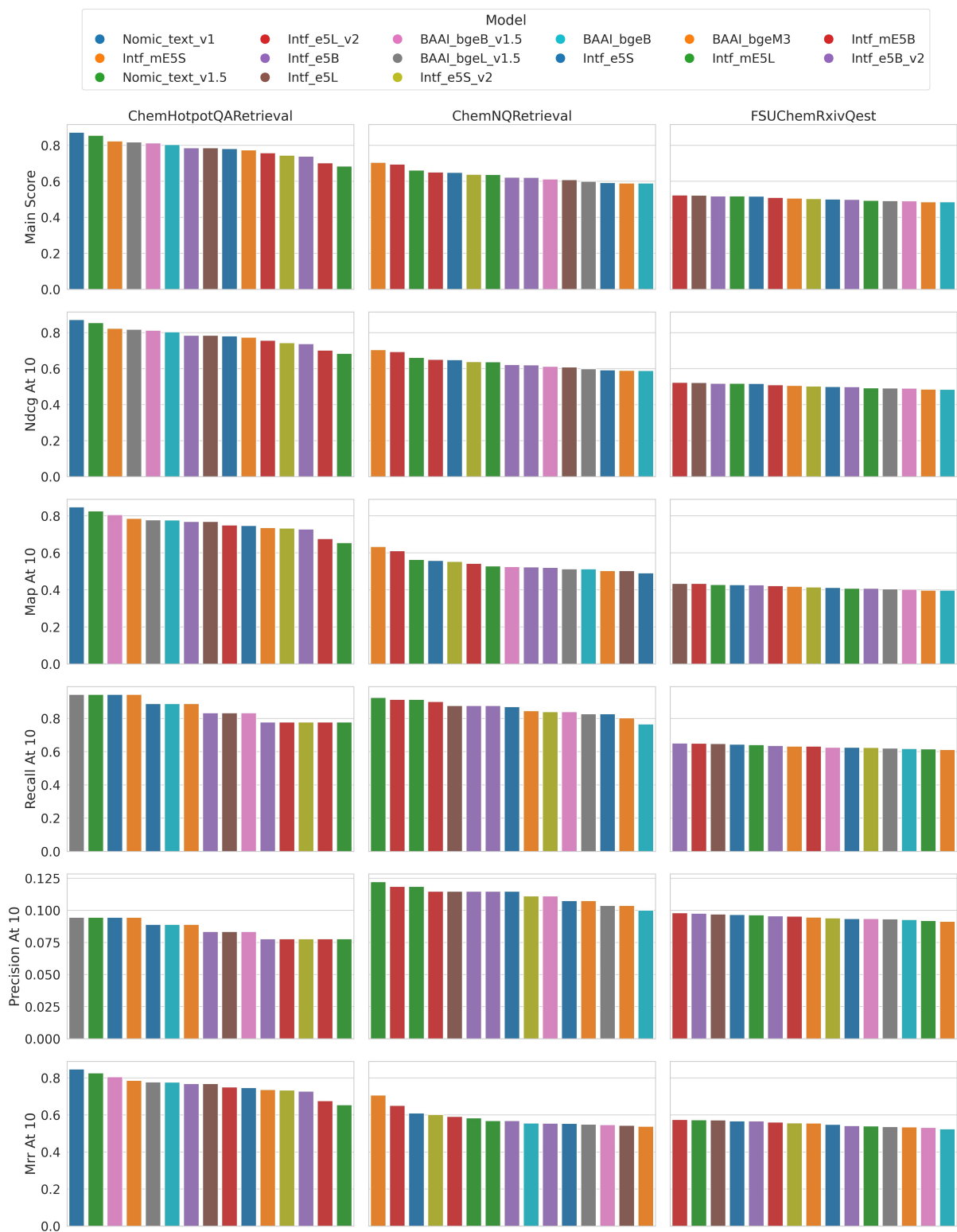


Figure 5: Comparison of the top-15 embedding models across three chemistry retrieval tasks—*ChemHotpotQARetrieval*, *ChemNQRetrieval*, and *FSUChemRxivQuest*—and six evaluation metrics: Main Score, NDCG@10, MAP@10, Recall@10, Precision@10, and MRR@10. Models are sorted by performance per task and metric.

Precision–recall dynamics, illustrated in Figure 6, reveal that models achieving high F_2

scores tend to strike a balance between coverage and specificity. The upper-right region of these scatter plots, which represents the ideal balance between precision and recall, is consistently occupied by retrieval-optimized models. This pattern confirms that models fine-tuned for retrieval tasks are better able to manage the inherent trade-off between retrieving broadly and retrieving accurately.

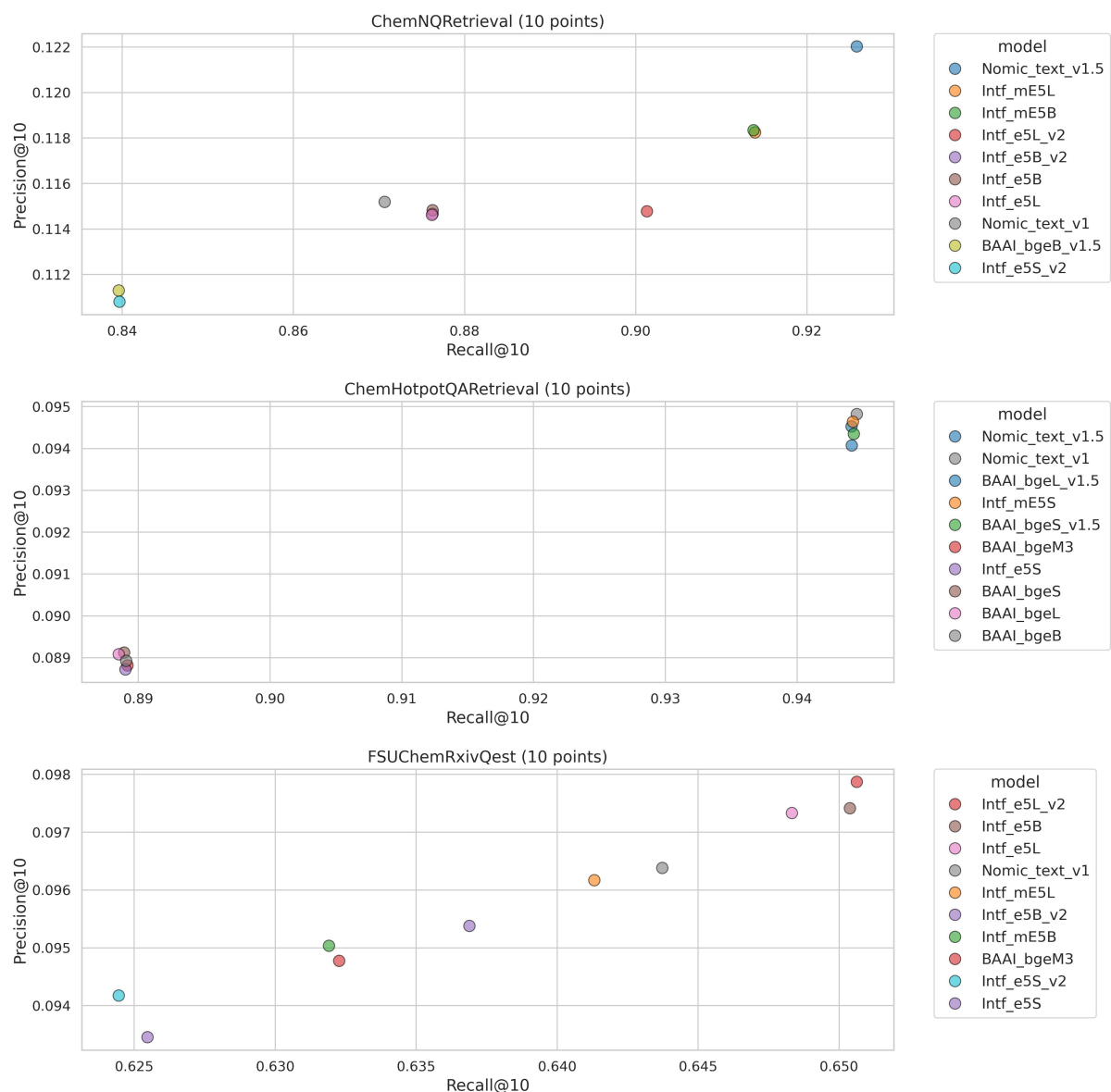


Figure 6: Scatter plots of Precision@10 vs Recall@10 for the top 10 models per dataset, ranked by F_2 score. Each subplot corresponds to a different chemistry retrieval task: *ChemNQRetrieval*, *ChemHotpotQARetrieval*, and *FSUChemRxivQest*.

Notably, this trade-off varies significantly by dataset. On the *ChemHotpotQARetrieval* and *ChemNQRetrieval* benchmarks, models such as *Nomic_text_v1.5* and *BAAI_bgeB_v1.5* achieve recall levels above 0.94, compensating for modest precision drops and yielding the highest F_2 scores. In contrast, on *FSUChemRxivQest*, which contains linguistically noisier content drawn from preprints, high recall models suffer pronounced drops in precision. Here,

the best performing model is `Intfloat_e5L_v2`, which, despite a recall approximately seven percentage points lower than the leaders, achieved the highest precision (0.098) and consequently the best F_2 score (0.306) for that benchmark.

Table 4: Top three embedding models per dataset based on F_2 score, which emphasizes recall. Each row shows the best-performing models for a given dataset. The final row reports the overall top 3 models by average F_2 score.

Dataset	Top Model 1	Top Model 2	Top Model 3
ChemNQRetrieval	Nomic_text_v1.5 (0.40)	Intf_mE5L (0.39)	Intf_mE5B (0.39)
ChemHotpotQARetrieval	Nomic_text_v1.5 (0.34)	Nomic_text_v1 (0.34)	BAAI_bgeL_v1.5 (0.34)
FSUChemRxivQest	Intf_e5L_v2 (0.31)	Intf_e5B (0.31)	Intf_e5L (0.30)
Overall	Nomic_text_v1.5 (0.37)	BAAI_bgeB_v1.5 (0.36)	Intf_mE5L (0.35)

This divergence suggests that the effectiveness of an embedding model is not absolute but contingent upon document type and linguistic regularity. Figure 7 provides further evidence of task-dependent behavior, showing that the range and spread of model performance vary substantially across benchmarks. *ChemHotpotQARetrieval* displays the widest interquartile range and the largest overall score gap between best- and worst-performing models, indicating that it is the most sensitive to embedding quality and perhaps the most challenging task.

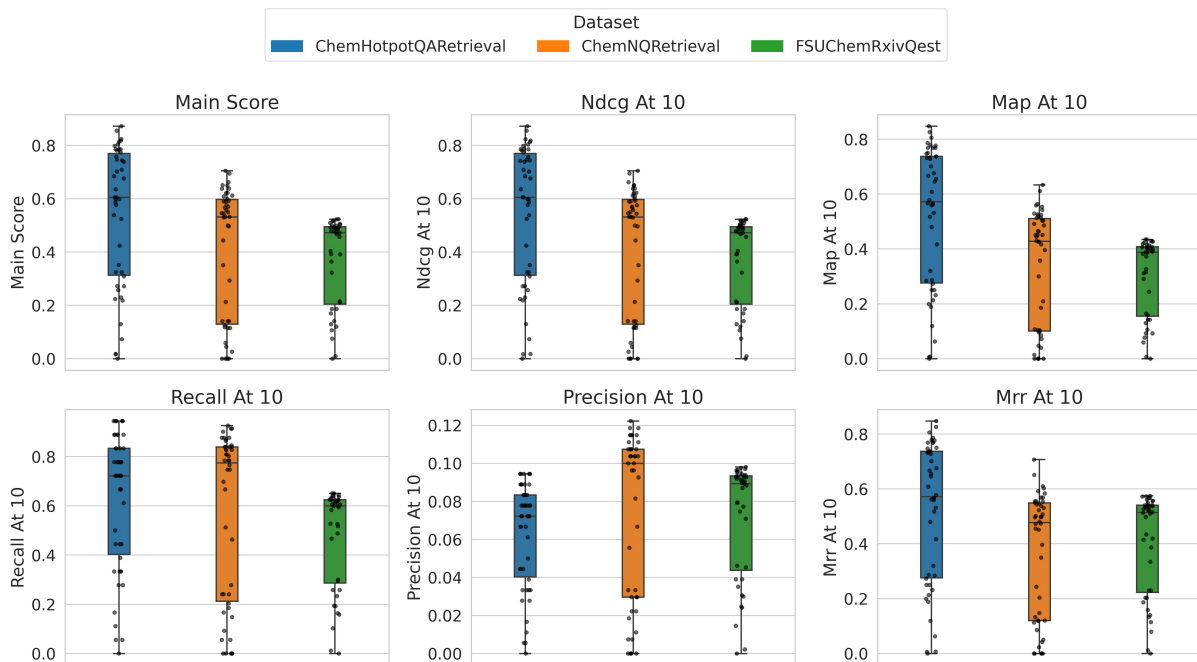


Figure 7: Distribution of model performance across three chemistry-focused retrieval tasks—*ChemHotpotQARetrieval*, *ChemNQRetrieval*, and *FSUChemRxivQest*—evaluated over six standard metrics. Each boxplot shows the spread and central tendency of model scores, with dot overlays representing individual models.

In contrast, *FSUChemRxivQest* yields better model separation in precision–recall space, enabling clearer differentiation among competing models and making it well-suited for evaluating fine-grained improvements in embedding architectures or training strategies. Table 5

Table 6: Embedding models belonging to the best-performing cluster, identified via PCA and k -means clustering on mean retrieval metrics. This cluster achieved the highest average performance across all metrics.

Top Model 1	Top Model 2	Top Model 3	Top Model 4	Top Model 5
Nomic_text_v1 (0.58)	Intf_mE5S (0.57)	Nomic_text_v1.5 (0.57)	Intf_e5L_v2 (0.56)	Intf_e5B (0.55)
Intf_e5L (0.54)	BAAI_bgeL_v1.5 (0.54)	BAAI_bgeB_v1.5 (0.54)	Intf_e5S (0.53)	Intf_e5S_v2 (0.53)
BAAI_bgeB (0.53)	BAAI_bgeM3 (0.53)	Intf_mE5L (0.53)	Intf_mE5B (0.53)	Intf_e5B_v2 (0.53)
BAAI_bgeL (0.53)	HKU_InstructXL (0.52)	BAAI_bgeS_v1.5 (0.50)		

From a practical standpoint, these findings indicate that retrieval-optimized encoders significantly outperform domain-specific but general-purpose models. The choice of embedding model alone can explain over 35 percentage points of variance in Main Score across tasks—comparable to the chunking strategy variance shown in Section 2.3. Architectures that excel on curated QA benchmarks may underperform on noisy scientific text, and vice versa. Therefore, hybrid pipelines—such as combining a high-recall encoder with a precision-oriented reranker—may offer improved robustness in real-world retrieval pipelines.

In summary, embedding evaluation reveals a two-dimensional optimization space for chemistry retrieval: chunking for context retention and embedding selection for semantic relevance. Recall has already saturated on certain benchmarks, meaning future improvements may arise primarily through gains in precision and ranking quality. Embedding model selection is thus not merely a technical detail but a decisive factor in system-level retrieval performance.

4 Methodology

This section describes the datasets, chunking strategies, embedding models, evaluation tasks, and retrieval pipeline used to assess the impact of chunking and embedding methods in retrieval-augmented generation (RAG) systems tailored for chemistry-related documents.

4.1 ChemRxivQuest

Our study is built on ChemRxivQuest[18], a curated and validated dataset comprising 970 high-quality question–answer (QA) pairs derived from 155 ChemRxiv preprints across 17 chemical subfields. Each QA pair is explicitly linked to its source paragraph, ensuring semantic traceability and contextual alignment. The dataset spans a diverse range of chemistry topics, including organic synthesis, catalysis, materials science, and theoretical chemistry, and covers a balanced distribution of conceptual, mechanistic, applied, and experimental questions. The dataset was constructed using an automated pipeline combining optical character recognition (OCR), QA pair generation via GPT-4o, and a fuzzy string-matching verification stage to ensure source-grounded accuracy. Full construction details are described in [18], where the authors provide a comprehensive analysis of the dataset’s structure and utility for chemistry-specific NLP.

4.2 text-embedding-3-large

OpenAI’s text-embedding-3-large model represents a significant advancement in text representation for retrieval tasks, offering robust semantic understanding across domains, including technical and scientific literature such as chemistry. With a high-dimensional embedding space (3072 dimensions), the model captures nuanced semantic relationships, which is particularly advantageous for disambiguating complex terminology and contextual usage common in chemical texts. Benchmark evaluations have shown that it outperforms its predecessor, text-embedding-ada-002, with improvements on standard datasets such as MTEB (64.6% vs. 61.0%) and multilingual retrieval (MIRACL), where it nearly doubles the performance (54.9% vs. 31.4%) [86]. Its ability to maintain competitive accuracy even at reduced dimensions, thanks to Matryoshka Representation Learning (MRL), makes it computationally efficient for large-scale retrieval systems. These qualities make text-embedding-3-large a strong candidate for domain-specific retrieval tasks in chemistry, where semantic precision and generalization are critical. By fixing the embedding model across all chunking configurations, we follow best practice as recommended by [11] to isolate pre-processing effects from representational factors.

4.3 chunking evaluation methods

To rigorously evaluate the effectiveness of various text chunking strategies in retrieval-based systems, we developed a comprehensive and extensible evaluation framework. This system is designed to assess how different chunking methods affect the retrievability of semantically relevant content from large corpora. The evaluation pipeline operates by segmenting textual documents into smaller units, embedding those segments into vector space, and then measuring how well they support the retrieval of ground-truth answer spans given natural language questions.

The framework accepts a corpus of plain text files as input, along with a corresponding dataset of natural language queries and their manually annotated answer spans. Each question in this dataset is associated with a specific document and includes one or more reference excerpts, each annotated with start and end character indices to define the relevant answer span. This setup allows for a granular, token-level evaluation of retrieval performance.

Once chunking is complete, the resulting segments are embedded using a configurable embedding model. The framework uses OpenAI’s text-embedding-3-large. Each embedded chunk is stored in a high-performance vector store that supports approximate nearest-neighbor search. Queries are also embedded, and their vector representations are used to retrieve the top- k most similar chunks from the database.

The evaluation then compares the retrieved chunks to the ground truth spans provided in the question dataset. All evaluations are run per chunking strategy, and the results are serialized into human-readable JSON files. Each output contains global averages for the metrics, as well as corpus-specific breakdowns to facilitate fine-grained analysis. This structure enables

robust comparisons across chunking configurations, such as varying chunk sizes or overlaps, and supports empirical justification for chunking choices in retrieval-augmented generation (RAG) systems.

4.4 Chunking Methods

Retrieval-Augmented Generation (RAG) systems depend critically on how source documents are segmented into manageable units or “chunks” prior to retrieval. Chunk boundaries not only determine what content is retrievable, but also influence the factual and contextual quality of generated answers. However, most chunking strategies used in practice are generic and not optimized for technical or scientific texts, such as those found in chemistry. To address this, we systematically evaluate a range of chunking methods—spanning from rule-based to neural and LLM-driven approaches—with the goal of understanding their impact on RAG system performance in a domain requiring high topical precision and semantic fidelity.

All methods examined in this study operate within the framework of OpenAI’s `cl100k` tokenizer to ensure token-level consistency across retrieval and generation stages. We apply these methods to *ChemRxivQuest* [18], a domain-specific corpus of curated chemistry-related documents, thereby grounding our evaluation in realistic, information-dense content.

We begin with classical strategies that prioritize speed and structural regularity. The **Fixed-Token-Chunker** segments text into fixed-size windows based purely on token count, optionally with overlap. While this method is efficient and easy to implement, it disregards semantic or syntactic structure, often resulting in fragmented thoughts and sentence breaks that degrade retrieval precision. The **Recursive-Token-Chunker**, by contrast, introduces hierarchical segmentation based on a prioritized set of textual delimiters. Originally proposed in LangChain [20], this method splits text recursively using a sequence of separators—typically newlines and whitespace—until the desired chunk size is reached. Following the enhancements suggested by Smith et al. [11], we adopt a modified hierarchy: [“\n\n”, “\n”, “.”, “?”, “!”, “ ”, “”]. This change introduces basic syntactic awareness, enabling cleaner sentence-aligned splits that reduce the frequency of semantically incoherent chunks.

To incorporate deeper semantic structure, we evaluate embedding-based chunking methods that use dense vector representations to detect topic shifts. The **Kamradt-Semantic-Chunker** [21] begins with sentence-level segmentation and computes embeddings for overlapping token windows. By analyzing the cosine similarity between adjacent embeddings, the method identifies chunk boundaries at points of significant semantic discontinuity. Typically, the 95th percentile of similarity drop is used as a threshold to trigger segmentation. This strategy yields variable-length chunks that better align with topical units, though it lacks mechanisms to ensure compliance with model-specific token constraints—an important limitation in real-world RAG pipelines.

To address this, a modified version—**Kamradt-Modified-Chunker** [11]—was proposed,

combining semantic segmentation with strict size control. It preserves the similarity-based boundary detection but introduces a binary search algorithm to adjust the threshold dynamically, ensuring that no chunk exceeds a pre-defined token limit. This method strikes a practical balance between semantic coherence and adherence to model context window limitations, making it better suited for transformer-based systems operating in constrained environments.

Another approach that emphasizes global cohesion is the **Cluster-Semantic-Chunker** [11], which reframes chunking as a global optimization problem. Initially, a document is divided into fine-grained segments of around 50 tokens using basic delimiters. Each segment is embedded independently, and a dynamic programming algorithm is employed to group these segments into chunks that maximize the overall intra-chunk semantic similarity. This yields highly coherent chunks that preserve broader thematic continuity, but the method is computationally intensive, rendering it less suitable for large-scale or streaming applications.

Lastly, we explore the **LLM-Semantic-Chunker**, a prompting-based method that leverages large language models to infer chunk boundaries directly [11]. Here, the input text is split into small spans—typically around 50 tokens—each bracketed with boundary markers. The annotated text is then passed to an LLM such as GPT-4o, which is prompted to identify semantically appropriate break points. Unlike embedding-based techniques that rely on static similarity thresholds, this method benefits from the model’s deep, contextual understanding of language and topic structure. While it often produces highly coherent and human-aligned chunks, it is also the most resource-intensive approach due to reliance on autoregressive inference and limited parallelizability.

These five methods represent diverse philosophies of chunking—ranging from purely lexical and syntactic heuristics to semantically informed neural and LLM-driven techniques. By applying them to the *ChemRxivQuest* dataset and evaluating their downstream performance in retrieval tasks, we examine how differences in chunk granularity, boundary sensitivity, and semantic continuity influence the overall effectiveness of RAG systems in scientific domains. The results of our analysis offer practical guidance for selecting or designing chunking pipelines that prioritize both computational efficiency and contextual accuracy in domain-specific applications.

4.5 Evaluation Metrics

We employ a comprehensive suite of evaluation metrics to assess both embedding model performance on retrieval tasks and the effectiveness of different chunking strategies for span-based matching. These metrics are categorized into three groups: (1) Information Retrieval Metrics, (2) Chunking and Span Matching Metrics, and (3) Cross-Task Performance Variability Metrics.

4.5.1 Information Retrieval Metrics

Information retrieval (IR) metrics are used to quantify the quality of the ranked document lists returned by embedding models in response to chemistry-related queries. Each metric emphasizes different aspects of relevance, ranking, and retrieval efficiency.

Mean Average Precision at 10 (MAP@10): MAP@10 evaluates the average precision of the top 10 results for each query and then averages it across all queries. It rewards systems that retrieve relevant documents early in the ranked list and penalizes those that interleave relevant and irrelevant results. It is defined as:

$$\text{MAP@10} = \frac{1}{|Q|} \sum_{q=1}^{|Q|} \left(\frac{1}{\min(R_q, 10)} \sum_{k=1}^{10} P_q(k) \cdot \text{rel}_q(k) \right)$$

where Q is the set of all queries, $P_q(k)$ is the precision at rank k for query q , $\text{rel}_q(k)$ is a binary indicator of relevance at rank k , and R_q is the number of relevant documents for query q .

Mean Reciprocal Rank at 10 (MRR@10): MRR@10 measures how early the first relevant document appears in the top 10 results. A higher score indicates that relevant results are ranked earlier, improving user experience. It is computed as:

$$\text{MRR@10} = \frac{1}{|Q|} \sum_{q=1}^{|Q|} \frac{1}{\text{rank}_q}$$

where rank_q is the position of the first relevant document for query q .

Normalized Discounted Cumulative Gain at 10 (NDCG@10): NDCG@10 evaluates both the relevance and rank position of results, giving higher weights to relevant documents that appear earlier in the ranking. Unlike MAP, it supports graded relevance if available.

$$\text{DCG}_q@10 = \sum_{i=1}^{10} \frac{2^{\text{rel}_i} - 1}{\log_2(i + 1)}, \quad \text{NDCG@10} = \frac{\text{DCG}_q@10}{\text{IDCG}_q@10}$$

where rel_i is the relevance score of the document at position i , and $\text{IDCG}_q@10$ is the ideal DCG for query q , used for normalization.

Precision@10: Precision@10 measures the fraction of the top 10 retrieved documents that are relevant. It provides a simple, interpretable metric for top-ranked precision:

$$\text{Precision@10} = \frac{|\text{Relevant}_q \cap \text{Retrieved}_q^{(10)}|}{10}$$

Recall@10: Recall@10 quantifies the ability of the system to retrieve all relevant documents, considering only the top 10 results:

$$\text{Recall@10} = \frac{|\text{Relevant}_q \cap \text{Retrieved}_q^{(10)}|}{|\text{Relevant}_q|}$$

Main Score: For each task, we designate a “Main Score” — typically the most representative or task-relevant IR metric (e.g., NDCG@10 for ranking-sensitive tasks or MAP@10 for relevance-focused tasks). This scalar score is used for summary comparisons across models.

4.5.2 Chunking and Span Matching Metrics

For evaluating the chunking strategies that extract spans from long texts (e.g., passages, abstracts), we use metrics that assess how well the predicted spans align with annotated ground truth spans.

Precision: The proportion of predicted spans that correctly match a gold-standard span (i.e., true positives divided by all positive predictions):

$$\text{Precision} = \frac{|\text{True Positives}|}{|\text{True Positives}| + |\text{False Positives}|}$$

Recall: The proportion of ground truth spans that were successfully identified:

$$\text{Recall} = \frac{|\text{True Positives}|}{|\text{True Positives}| + |\text{False Negatives}|}$$

F_1 Score: A harmonic mean of precision and recall, used when both false positives and false negatives are equally undesirable:

$$F_1 = 2 \cdot \frac{\text{Precision} \cdot \text{Recall}}{\text{Precision} + \text{Recall}}$$

F_2 Score: A variant of the F-score that weights recall more heavily, suitable for scenarios where missing relevant spans is more costly than retrieving extra ones:

$$F_2 = 5 \cdot \frac{\text{Precision} \cdot \text{Recall}}{4 \cdot \text{Precision} + \text{Recall}}$$

Intersection over Union (IoU): Used to measure the overlap between predicted and true spans. IoU is particularly useful for evaluating the boundary alignment of spans:

$$\text{IoU} = \frac{|\text{Prediction} \cap \text{Ground Truth}|}{|\text{Prediction} \cup \text{Ground Truth}|}$$

Precision@ Ω : This metric evaluates the precision of predictions under a constraint Ω , such as a distance threshold (e.g., matching spans within a 10-token window). It reflects task-specific tolerances for span alignment:

$$\text{Precision@}\Omega = \frac{|\text{Correct Predictions under } \Omega|}{|\text{Total Predictions under } \Omega|}$$

4.5.3 Cross-Task Performance Variability Metrics

To understand the consistency and robustness of embedding models across multiple tasks, we report statistics that describe performance variability:

Median Main Score: The median score achieved by all models on a particular task, offering a robust central tendency measure that is less sensitive to outliers.

Interquartile Range (IQR): The spread between the 25th and 75th percentile scores for each task, quantifying the variability of model performance:

$$\text{IQR} = Q_3 - Q_1$$

Best–Worst Δ : The difference between the highest and lowest scores for a given task, indicating the maximum spread in performance:

$$\Delta = \text{Best Model Score} - \text{Worst Model Score}$$

This metric highlights tasks where model performance is either tightly clustered (low Δ) or highly variable (high Δ), indicating potential task difficulty or model sensitivity.

4.6 Massive Text Embedding Benchmark (MTEB)

The Massive Text Embedding Benchmark (MTEB) [17] provides a systematic and comprehensive framework for evaluating dense text representations across a diverse array of natural language processing (NLP) tasks, with a particular emphasis on retrieval. Within the MTEB framework, dense retrieval serves as the primary evaluation paradigm, wherein both queries and documents are independently encoded into dense vector embeddings using pre-trained transformer-based encoder models. These embeddings are normalized to unit length to facilitate similarity comparisons via cosine similarity. Retrieval is implemented using exact nearest-neighbor search, where the cosine similarities between normalized query and document embeddings are computed through matrix multiplication. This approach ensures both computational efficiency and ranking precision, particularly for small to medium-sized datasets. Performance

is assessed using a suite of standard information retrieval metrics, including Normalized Discounted Cumulative Gain at rank 10 (nDCG@10), Mean Average Precision (MAP), Recall@k, Precision@k, and Mean Reciprocal Rank (MRR@k). Together, these provide a robust and multifaceted evaluation of dense embedding effectiveness in semantic retrieval tasks.

4.7 External Chemistry Retrieval Tasks

To evaluate the generalisability of embedding models across diverse chemistry-related information retrieval scenarios, we additionally benchmark all models on three established chemistry-focused retrieval tasks from the Massive Text Embedding Benchmark (MTEB). These datasets are publicly available via Hugging Face and have been curated to support domain-specific evaluation.

ChemHotpotQARetrieval⁴ is a multi-hop retrieval task derived from the HotpotQA⁵ dataset, which consists of question-answer pairs sourced from English Wikipedia. For this chemistry-specific subset, questions were filtered by identifying entries within the chemistry category and traversing linked articles up to three levels deep. This subset emphasizes multi-hop reasoning over several documents to answer conceptual and mechanistic questions in chemistry.

ChemNQRetrieval⁶ is based on the Chemistry Natural Questions subset of the Natural Questions dataset⁷, which contains real user queries issued to Google and grounded in Wikipedia content. Similar to ChemHotpotQA, chemistry-related questions were extracted through a structured traversal of Wikipedia’s chemistry category and its linked pages. This dataset reflects real-world information needs in an open-domain chemistry context.

These tasks collectively span a range of retrieval challenges—from multi-hop document reasoning to precise entity-level matching—providing a comprehensive benchmark suite for assessing the robustness and transferability of embedding models in the chemical domain. In this paper, we introduce **FSUChemRxivQuest**, a new MTEB-formatted [17] task derived from chemistry preprints.

4.8 Methodology for generating FSUChemRxivQuest

The benchmark includes 970 natural language queries that reflect typical chemistry research inquiries, covering diverse topics like organic synthesis, materials science, and chemical theory. The corpus comprises 32,698 paragraph-level text chunks, carefully extracted to maintain semantic coherence and scientific relevance. FSUChemRxivQuest provides 1,545 query-passage relevance pairs, enabling evaluation under realistic multi-positive retrieval scenarios.

The dataset is distributed as JSONL files: `queries.jsonl` (queries and metadata),

⁴<https://huggingface.co/datasets/BASF-AI/ChemHotpotQARetrieval>

⁵<https://huggingface.co/datasets/mteb/hotpotqa>

⁶<https://huggingface.co/datasets/BASF-AI/ChemNQRetrieval>

⁷<https://huggingface.co/datasets/mteb/nq>

corpus.jsonl (corpus chunks), and qrels/test.jsonl (test relevance judgments), adhering to MTEB specifications. Released under a CC BY 4.0 license, FSUChemRxivQuest addresses the need for domain-specific retrieval benchmarks, fostering improved dense retrieval models for scientific document retrieval in chemistry.

5 Discussion

This study presents the first large-scale, systematic evaluation of chunking strategies and embedding models for retrieval-augmented generation (RAG) systems within the chemical sciences. Our findings demonstrate that segmentation configuration is not merely a preprocessing detail, but a critical design choice with substantial consequences for retrieval effectiveness.

5.1 Impact of Chunking on Retrieval Quality

Our results reveal that recursive token-based chunking—particularly the R100-0 configuration—consistently outperforms alternative methods across key metrics such as precision, recall, and span alignment. Recursive strategies preserve semantic integrity by leveraging syntactic cues, allowing the system to maintain meaningful context without including extraneous content. Compared to the best-performing fixed-span method, FX64-12, recursive methods achieve up to 45% higher domain-weighted precision (Precision_Ω).

Overlap analysis further shows that chunking strategies with no or minimal overlap strike the best balance between retrieval quality and computational cost. Although increased overlap improves recall marginally, it significantly reduces precision and expands index size, making it impractical for precision-sensitive applications.

5.2 Embedding Model Selection in Context

Embedding model evaluations indicate that retrieval-tuned encoders—such as Nomic_text_v1.5, BAAI_bgeB_v1.5, and Intfloat_e5L_v2—substantially outperform both general-purpose and domain-specialized models like SciBERT. This finding challenges the assumption that domain pretraining alone ensures optimal performance. Instead, models trained with contrastive retrieval objectives offer better precision–recall trade-offs and generalize more effectively across diverse chemistry retrieval tasks.

Moreover, model performance varies depending on task type and corpus structure. While Nomic_text_v1.5 leads in QA-style tasks with high recall, Intfloat_e5L_v2 excels in noisier or preprint-based benchmarks due to its higher precision. These distinctions suggest that model selection should be guided by both the retrieval context and the desired trade-off between precision and recall.

5.3 Chunking vs. Embedding: A Surprising Trade-Off

An important outcome of this work is the finding that chunking strategy has an impact on retrieval performance comparable to—and in some cases greater than—that of embedding model choice. While embedding model selection has received extensive attention, our results highlight a tenfold variation in IoU purely due to segmentation choices. This underscores the necessity of systematically evaluating chunking methods as a central design factor in RAG pipelines.

5.4 Practical Recommendations

Our results offer actionable guidelines for practitioners developing chemistry-aware RAG systems:

- Use recursive, non-overlapping chunking (R100-0) as a strong default strategy. It offers excellent performance with minimal indexing overhead.
- Prefer retrieval-optimized embeddings (e.g., Nomic, BGE, Intfloat E5) over general-purpose or domain-pretrained models unless additional fine-tuning is possible.
- Avoid high-overlap fixed-span chunking, which degrades precision without significant recall gains.
- Align embedding model selection with document type and task demands: precision-oriented models for noisy or unstructured corpora, recall-oriented models for curated datasets.

5.5 Limitations and Future Work

While this study establishes strong empirical baselines, several limitations should be acknowledged. Our experiments focus solely on the chemistry domain; future work should explore whether similar trends hold in other scientific fields such as materials science or biomedicine. Furthermore, although we evaluate a wide array of embeddings and chunking strategies, we do not investigate multimodal retrieval, reranking pipelines, or knowledge-augmented embeddings—all of which represent promising avenues for improvement.

Lastly, although R100-0 performs best across current benchmarks, specialized tasks (e.g., summarization, citation generation) may benefit from customized chunking heuristics. Future research could explore hybrid segmentation strategies, ensemble retrieval architectures, and generative accuracy of RAG outputs to further advance domain-specific language understanding in the sciences.

6 Conclusion

This work presents a comprehensive empirical analysis of chunking strategies and embedding models within retrieval-augmented generation pipelines designed for the chemical sciences. Our findings establish that chunking configurations can have as much—if not more—influence on retrieval quality as the choice of embedding model. Recursive, syntactically aware chunkers, especially R100-0, offer substantial improvements in both retrieval precision and stability across chemistry subdomains. On the representation front, we show that retrieval-tuned embeddings significantly outperform both general-purpose and domain-pretrained alternatives, challenging the assumption that domain specialization alone ensures superior performance. Through our introduction of *FSUChemRxivQuest* and benchmarking across three diverse retrieval tasks, we provide the community with robust evaluation tools and baselines. Ultimately, this study lays the groundwork for future chemistry-aware RAG development, emphasizing the importance of careful pre-processing and embedding model selection in high-precision scientific applications.

Acknowledgments

This work was supported by the Leibniz Institute of Photonic Technology and the Friedrich Schiller University Jena. We also acknowledge the developers of the Massive Text Embedding Benchmark (MTEB) framework and the open-source community for providing the embedding models and tools that made this evaluation possible.

References

- [1] Rosaria Ciriminna, Giuseppe Angellotti, Giovanna Li Petri, and Mario Pagliaro. Reproducibility in chemistry research. *Heliyon*, 10(14), 2024.
- [2] Patrick Lewis, Ethan Perez, Aleksandara Piktus, Fabio Petroni, Vladimir Karpukhin, Naman Goyal, Heinrich Kuttler, Mike Lewis, Wen tau Yih, Tim Rocktaschel, Sebastian Riedel, and Douwe Kiela. Retrieval-augmented generation for knowledge-intensive nlp tasks. *ArXiv*, abs/2005.11401, 2020. URL <https://api.semanticscholar.org/CorpusID:218869575>.
- [3] Yunfan Gao, Yun Xiong, Xinyu Gao, Kangxiang Jia, Jinliu Pan, Yuxi Bi, Yixin Dai, Jiawei Sun, Haofen Wang, and Haofen Wang. Retrieval-augmented generation for large language models: A survey. *arXiv preprint arXiv:2312.10997*, 2:1, 2023.
- [4] Michael D. Skarlinski, Sam Cox, Jon M. Laurent, James D. Braza, Michaela M. Hinks, M. Hammerling, Manvitha Ponnampati, Samuel Rodrigues, and Andrew D.

- White. Language agents achieve superhuman synthesis of scientific knowledge. *ArXiv*, abs/2409.13740, 2024. URL <https://api.semanticscholar.org/CorpusId:272827223>.
- [5] Philippe Schwaller. Chemlit-qa: a human evaluated dataset for chemistry rag tasks. *MACHINE LEARNING-SCIENCE AND TECHNOLOGY*, 6(2), 2025.
- [6] Xianrui Zhong, Bowen Jin, Siru Ouyang, Yanzhen Shen, Qiao Jin, Yin Fang, Zhiyong Lu, and Jiawei Han. Benchmarking retrieval-augmented generation for chemistry. *arXiv preprint arXiv:2505.07671*, 2025.
- [7] Namkyeong Lee, Edward De Brouwer, Ehsan Hajiramezanali, Tommaso Biancalani, Chanyoung Park, and Gabriele Scalia. Rag-enhanced collaborative llm agents for drug discovery. *arXiv preprint arXiv:2502.17506*, 2025.
- [8] Nicholas Matsumoto, Jay Moran, Hyunjun Choi, Miguel E Hernandez, Mythreya Venkatesan, Paul Wang, and Jason H Moore. Kragen: a knowledge graph-enhanced rag framework for biomedical problem solving using large language models. *Bioinformatics*, 40(6):btae353, 2024.
- [9] Antonio Jimeno Yepes, Yao You, Jan Milczek, Sebastian Laverde, and Renyu Li. Financial report chunking for effective retrieval augmented generation. *arXiv preprint arXiv:2402.05131*, 2024.
- [10] Rajvardhan Patil, Sorio Boit, Venkat Gudivada, and Jagadeesh Nandigam. A survey of text representation and embedding techniques in nlp. *IEEE Access*, 11:36120–36146, 2023.
- [11] Brandon Smith and Anton Troynikov. Evaluating chunking strategies for retrieval. Technical report, Chroma, July 2024. URL <https://research.trychroma.com/evaluating-chunking>. Chroma Technical Report.
- [12] Ali Shirae Kasmaee, Mohammad Khodadad, Mohammad Arshi Saloot, Nicholas Sherck, Stephen Dokas, Hamidreza Mahyar, and Soheila Samiee. Chemteb: Chemical text embedding benchmark, an overview of embedding models performance & efficiency on a specific domain. *arXiv preprint arXiv:2412.00532*, 2024.
- [13] Tom Kwiatkowski, Jennimaria Palomaki, Olivia Redfield, Michael Collins, Ankur Parikh, Chris Alberti, Danielle Epstein, Illia Polosukhin, Jacob Devlin, Kenton Lee, et al. Natural questions: a benchmark for question answering research. *Transactions of the Association for Computational Linguistics*, 7:453–466, 2019.

- [14] Tri Nguyen, Mir Rosenberg, Xia Song, Jianfeng Gao, Saurabh Tiwary, Rangan Majumder, and Li Deng. Ms marco: A human-generated machine reading comprehension dataset. 2016.
- [15] Zhilin Yang, Peng Qi, Saizheng Zhang, Yoshua Bengio, William Cohen, Ruslan Salakhutdinov, and Christopher D. Manning. HotpotQA: A dataset for diverse, explainable multi-hop question answering. In Ellen Riloff, David Chiang, Julia Hockenmaier, and Jun’ichi Tsujii, editors, *Proceedings of the 2018 Conference on Empirical Methods in Natural Language Processing*, pages 2369–2380, Brussels, Belgium, October–November 2018. Association for Computational Linguistics. doi: 10.18653/v1/D18-1259. URL <https://aclanthology.org/D18-1259>.
- [16] Kenneth Enevoldsen, Isaac Chung, Imene Kerboua, Márton Kardos, Ashwin Mathur, David Stap, Jay Gala, Wissam Sibli, Dominik Krzemiński, Genta Indra Winata, Saba Sturua, Saiteja Utpala, Mathieu Ciancone, Marion Schaeffer, Gabriel Sequeira, Diganta Misra, Shreeya Dhakal, Jonathan Rystrom, Roman Solomatin, Ömer Çağatan, Akash Kundu, Martin Bernstorff, Shitao Xiao, Akshita Sukhlecha, Bhavish Pahwa, Rafał Poświata, Kranthi Kiran GV, Shawon Ashraf, Daniel Auras, Björn Plüster, Jan Philipp Harries, Loïc Magne, Isabelle Mohr, Mariya Hendriksen, Dawei Zhu, Hippolyte Gisserot-Boukhlef, Tom Aarsen, Jan Kostkan, Konrad Wojtasik, Taemin Lee, Marek Šuppa, Crystina Zhang, Roberta Rocca, Mohammed Hamdy, Andrianos Michail, John Yang, Manuel Faysse, Aleksei Vatolin, Nandan Thakur, Manan Dey, Dipam Vasani, Pranjal Chitale, Simone Tedeschi, Nguyen Tai, Artem Snegirev, Michael Günther, Mengzhou Xia, Weijia Shi, Xing Han Lù, Jordan Clive, Gayatri Krishnakumar, Anna Maksimova, Silvan Wehrli, Maria Tikhonova, Henil Panchal, Aleksandr Abramov, Malte Ostendorff, Zheng Liu, Simon Clematide, Lester James Miranda, Alena Fenogenova, Guangyu Song, Ruqiya Bin Safi, Wen-Ding Li, Alessia Borghini, Federico Cassano, Hongjin Su, Jimmy Lin, Howard Yen, Lasse Hansen, Sara Hooker, Chenghao Xiao, Vaibhav Adlakha, Orion Weller, Siva Reddy, and Niklas Muennighoff. Mmteb: Massive multilingual text embedding benchmark. *arXiv preprint arXiv:2502.13595*, 2025. doi: 10.48550/arXiv.2502.13595. URL <https://arxiv.org/abs/2502.13595>.
- [17] Niklas Muennighoff, Nouamane Tazi, Loic Magne, and Nils Reimers. Mteb: Massive text embedding benchmark. *arXiv preprint arXiv:2210.07316*, 2022.
- [18] Mahmoud Amiri and Thomas Bocklitz. Chemrxivquest: A curated chemistry question-answer database extracted from chemrxiv preprints. *arXiv preprint arXiv:2505.05232*, 2025.
- [19] Aryan Jadon and Avinash Patil. A comprehensive survey of evaluation techniques for recommendation systems. In *International Conference on Computation of Artificial Intelligence & Machine Learning*, pages 281–304. Springer, 2024.

- [20] Harrison Chase and LangChain contributors. Langchain: Building applications with llms through composability. <https://github.com/langchain-ai/langchain>, 2022. Accessed: 2025-05-28.
- [21] Greg Kamradt. 5 levels of text splitting. https://github.com/FullStackRetrieval-com/RetrievalTutorials/blob/main/tutorials/LevelsOfTextSplitting/5_Levels_Of_Text_Splitting.ipynb, 2024. Implementation of Semantic Chunking.
- [22] Nils Reimers and Iryna Gurevych. all-minilm-l6-v2. <https://huggingface.co/sentence-transformers/all-MiniLM-L6-v2>, 2021.
- [23] Nils Reimers and Iryna Gurevych. Sentence-bert: Sentence embeddings using siamese bert-networks. *arXiv preprint arXiv:1908.10084*, 2019.
- [24] Nils Reimers and Iryna Gurevych. all-minilm-l12-v2. <https://huggingface.co/sentence-transformers/all-MiniLM-L12-v2>, 2021.
- [25] Nils Reimers and Iryna Gurevych. all-mpnet-base-v2. <https://huggingface.co/sentence-transformers/all-mpnet-base-v2>, 2021.
- [26] Nils Reimers and Iryna Gurevych. gtr-t5-base. <https://huggingface.co/sentence-transformers/gtr-t5-base>, 2021.
- [27] Nils Reimers and Iryna Gurevych. gtr-t5-large. <https://huggingface.co/sentence-transformers/gtr-t5-large>, 2021.
- [28] Nils Reimers and Iryna Gurevych. gtr-t5-xl. <https://huggingface.co/sentence-transformers/gtr-t5-xl>, 2021.
- [29] Nils Reimers and Iryna Gurevych. bert-base-nli-mean-tokens. <https://huggingface.co/sentence-transformers/bert-base-nli-mean-tokens>, 2019.
- [30] Nils Reimers and Iryna Gurevych. multi-qa-mpnet-base-dot-v1. <https://huggingface.co/sentence-transformers/multi-qa-mpnet-base-dot-v1>, 2021.
- [31] Nils Reimers and Iryna Gurevych. paraphrase-multilingual-minilm-l12-v2. <https://huggingface.co/sentence-transformers/paraphrase-multilingual-MiniLM-L12-v2>, 2020.
- [32] Nils Reimers and Iryna Gurevych. paraphrase-multilingual-mpnet-base-v2. <https://huggingface.co/sentence-transformers/paraphrase-multilingual-mpnet-base-v2>, 2021.

- [33] Yu Gu, Robert Tinn, Hao Cheng, Michael Lucas, Naoto Usuyama, Xiaodong Liu, Tristan Naumann, Jianfeng Gao, and Hoifung Poon. Domain-specific language model pretraining for biomedical natural language processing. *ACM Transactions on Computing for Healthcare (HEALTH)*, 3(1):1–23, 2021.
- [34] Yifan Gu, Rajesh Tinn, Hao Cheng, Michael Lucas, Naoto Usuyama, Xiaodong Liu, Tristan Naumann, Jianfeng Gao, and Hoifung Poon. Biomednlp-biomedbert-base-uncased-abstract-fulltext. <https://huggingface.co/microsoft/BiomedNLP-BiomedBERT-base-uncased-abstract-fulltext>, 2021.
- [35] Yifan Gu, Rajesh Tinn, Hao Cheng, Michael Lucas, Naoto Usuyama, Xiaodong Liu, Tristan Naumann, Jianfeng Gao, and Hoifung Poon. Biomednlp-biomedbert-base-uncased-abstract. <https://huggingface.co/microsoft/BiomedNLP-BiomedBERT-base-uncased-abstract>, 2021.
- [36] Yifan Gu, Rajesh Tinn, Hao Cheng, Michael Lucas, Naoto Usuyama, Xiaodong Liu, Tristan Naumann, Jianfeng Gao, and Hoifung Poon. Biomednlp-pubmedbert-base-uncased-abstract-fulltext. <https://huggingface.co/microsoft/BiomedNLP-PubMedBERT-base-uncased-abstract-fulltext>, 2021.
- [37] Yifan Gu, Rajesh Tinn, Hao Cheng, Michael Lucas, Naoto Usuyama, Xiaodong Liu, Tristan Naumann, Jianfeng Gao, and Hoifung Poon. Biomednlp-pubmedbert-base-uncased-abstract. <https://huggingface.co/microsoft/BiomedNLP-PubMedBERT-base-uncased-abstract>, 2021.
- [38] Wenhui Wang, Furu Wei, Li Dong, Hangbo Bao, Nan Yang, and Ming Zhou. Minilm: Deep self-attention distillation for task-agnostic compression of pre-trained transformers. *arXiv preprint arXiv:2002.10957*, 2020.
- [39] Siqi Wang, Furu Wei, Li Dong, Hangbo Bao, Nan Yang, and Ming Zhou. Minilm-l12-h384-uncased. <https://huggingface.co/microsoft/MiniLM-L12-H384-uncased>, 2020.
- [40] Kaitao Song, Xu Tan, Tao Qin, Jianfeng Lu, and Tie-Yan Liu. MpNet: Masked and permuted pre-training for language understanding. *arXiv preprint arXiv:2004.09297*, 2020.
- [41] Kaitao Song, Xu Tan, Tao Qin, Jianfeng Lu, and Tie-Yan Liu. mpnet-base. <https://huggingface.co/microsoft/mpnet-base>, 2020.
- [42] Liang Wang, Nan Yang, Xiaolong Huang, Binxing Jiao, Linjun Yang, Daxin Jiang, Rangan Majumder, and Furu Wei. Text embeddings by weakly-supervised contrastive pre-training. *arXiv preprint arXiv:2212.03533*, 2022.

- [43] Luyu Wang, Yuwei Zhou, Xiang Ren, Julian McAuley, and Yiming Yang. e5-small. <https://huggingface.co/intfloat/e5-small>, 2022.
- [44] Luyu Wang, Yuwei Zhou, Xiang Ren, Jing Zhang, and Yiming Tao. e5-small-v2. <https://huggingface.co/intfloat/e5-small-v2>, 2022.
- [45] Luyu Wang, Yuwei Zhou, Xiang Ren, Jing Zhang, and Yiming Tao. e5-base. <https://huggingface.co/intfloat/e5-base>, 2022.
- [46] Luyu Wang, Yuwei Zhou, Xiang Ren, Jing Zhang, and Yiming Tao. e5-base-v2. <https://huggingface.co/intfloat/e5-base-v2>, 2022.
- [47] Luyu Wang, Yuwei Zhou, Xiang Ren, Jing Zhang, and Yiming Tao. e5-large. <https://huggingface.co/intfloat/e5-large>, 2022.
- [48] Luyu Wang, Yuwei Zhou, Xiang Ren, Jing Zhang, and Yiming Tao. e5-large-v2. <https://huggingface.co/intfloat/e5-large-v2>, 2022.
- [49] Luyu Wang, Yuwei Zhou, Xiang Ren, Jing Zhang, and Yiming Tao. multilingual-e5-base. <https://huggingface.co/intfloat/multilingual-e5-base>, 2022.
- [50] Luyu Wang, Yuwei Zhou, Xiang Ren, Jing Zhang, and Yiming Tao. multilingual-e5-large. <https://huggingface.co/intfloat/multilingual-e5-large>, 2022.
- [51] Luyu Wang, Yuwei Zhou, Xiang Ren, Jing Zhang, and Yiming Tao. multilingual-e5-small. <https://huggingface.co/intfloat/multilingual-e5-small>, 2022.
- [52] Shitao Xiao, Zheng Liu, Peitian Zhang, and Niklas Muennighoff. C-pack: Packaged resources to advance general chinese embedding, 2023.
- [53] Yue Liu, Yixin Wang, Yining Liu, Shuai Wang, Jiaze Xu, Zhiyuan Liu, and Jie Tang. bge-small-en. <https://huggingface.co/BAAI/bge-small-en>, 2023.
- [54] Yue Liu, Yixin Wang, Yining Liu, Shuai Wang, Jiaze Xu, Zhiyuan Liu, and Jie Tang. bge-small-en-v1.5. <https://huggingface.co/BAAI/bge-small-en-v1.5>, 2023.
- [55] Yue Liu, Yixin Wang, Yining Liu, Shuai Wang, Jiaze Xu, Zhiyuan Liu, and Jie Tang. bge-base-en. <https://huggingface.co/BAAI/bge-base-en>, 2023.
- [56] Yue Liu, Yixin Wang, Yining Liu, Shuai Wang, Jiaze Xu, Zhiyuan Liu, and Jie Tang. bge-base-en-v1.5. <https://huggingface.co/BAAI/bge-base-en-v1.5>, 2023.

- [57] Yue Liu, Yixin Wang, Yining Liu, Shuai Wang, Jiaze Xu, Zhiyuan Liu, and Jie Tang. bge-large-en. <https://huggingface.co/BAAI/bge-large-en>, 2023.
- [58] Yue Liu, Yixin Wang, Yining Liu, Shuai Wang, Jiaze Xu, Zhiyuan Liu, and Jie Tang. bge-large-en-v1.5. <https://huggingface.co/BAAI/bge-large-en-v1.5>, 2023.
- [59] Jianlv Chen, Shitao Xiao, Peitian Zhang, Kun Luo, Defu Lian, and Zheng Liu. Bge m3-embedding: Multi-lingual, multi-functionality, multi-granularity text embeddings through self-knowledge distillation, 2024.
- [60] Yue Liu, Yixin Wang, Yining Liu, Shuai Wang, Jiaze Xu, Zhiyuan Liu, and Jie Tang. bge-m3. <https://huggingface.co/BAAI/bge-m3>, 2023.
- [61] Nomic AI. nomic-embed-text-v1. <https://huggingface.co/nomic-ai/nomic-embed-text-v1>, 2023.
- [62] Zach Nussbaum, John X. Morris, Brandon Duderstadt, and Andriy Mulyar. Nomic embed: Training a reproducible long context text embedder, 2024.
- [63] Nomic AI. nomic-embed-text-v1.5. <https://huggingface.co/nomic-ai/nomic-embed-text-v1.5>, 2024.
- [64] Nomic AI. nomic-bert-2048. <https://huggingface.co/nomic-ai/nomic-bert-2048>, 2023.
- [65] Noam Shazeer. Glu variants improve transformer. *arXiv preprint arXiv:2002.05202*, 2020.
- [66] Gautier Izacard, Mathilde Caron, Lucas Hosseini, Sebastian Riedel, Piotr Bojanowski, Armand Joulin, and Edouard Grave. Unsupervised dense information retrieval with contrastive learning. *arXiv preprint arXiv:2112.09118*, 2021.
- [67] Gautier Izacard, Marshall Grusky, Ehsan Hosseini-Asl, and Edouard Grave. contriever. <https://huggingface.co/facebook/contriever>, 2022.
- [68] Gautier Izacard, Marshall Grusky, Ehsan Hosseini-Asl, and Edouard Grave. contriever-msmarco. <https://huggingface.co/facebook/contriever-msmarco>, 2022.
- [69] Soham Chithrananda, Gabriel Grand, and Bharath Ramsundar. Chemberta: Large-scale self-supervised pretraining for molecular property prediction, 2020. Available at <https://arxiv.org/abs/2010.09885>.

- [70] DeepChem. Chemberta-77m-mtr. <https://huggingface.co/DeepChem/ChemBERTa-77M-MTR>, 2023.
- [71] Jacob Devlin, Ming-Wei Chang, Kenton Lee, and Kristina Toutanova. Bert: Pre-training of deep bidirectional transformers for language understanding. *arXiv preprint arXiv:1810.04805*, 2018.
- [72] Jina AI. jina-embeddings-v2-base-en. <https://huggingface.co/jinaai/jina-embeddings-v2-base-en>, 2023.
- [73] Michael Günther, Jackmin Ong, Isabelle Mohr, Alaeddine Abdessalem, Tanguy Abel, Mohammad Kalim Akram, Susana Guzman, Georgios Mastrapas, Saba Sturua, Bo Wang, Maximilian Werk, Nan Wang, and Han Xiao. Jina embeddings 2: 8192-token general-purpose text embeddings for long documents, 2023.
- [74] Jina AI. jina-embeddings-v2-small-en. <https://huggingface.co/jinaai/jina-embeddings-v2-small-en>, 2023.
- [75] Danish Rana, Alok Choudhary, and Ankit Agrawal. Matscibert: A materials domain language model. <https://huggingface.co/m3rg-iitd/matscibert>, 2021.
- [76] Tanishq Gupta, Mohd Zaki, N. M. Anoop Krishnan, and Mausam. MatSciBERT: A materials domain language model for text mining and information extraction. *npj Computational Materials*, 8(1):102, May 2022. ISSN 2057-3960. doi: 10.1038/s41524-022-00784-w. URL <https://www.nature.com/articles/s41524-022-00784-w>.
- [77] DescribeAI. Gemini: General embeddings from mixed-initiative instruction. <https://huggingface.co/describeai/gemini>, 2024.
- [78] Hanzi Wang, Yujia Zhou, Xiang Liu, and Minlie Huang. Instructor-xl: Teaching models with instruction and feedback. <https://huggingface.co/hkunlp/instructor-xl>, 2022.
- [79] Hongjin Su, Weijia Shi, Jungo Kasai, Yizhong Wang, Yushi Hu, Mari Ostendorf, Wentau Yih, Noah A Smith, Luke Zettlemoyer, and Tao Yu. One embedder, any task: Instruction-finetuned text embeddings. *arXiv preprint arXiv:2212.09741*, 2022.
- [80] Iz Beltagy, Kyle Lo, and Arman Cohan. Scibert: A pretrained language model for scientific text. *arXiv preprint arXiv:1903.10676*, 2019.
- [81] Iz Beltagy, Kyle Lo, and Arman Cohan. Scibert: A pretrained language model for scientific text. In *EMNLP*. Association for Computational Linguistics, 2019. URL <https://www.aclweb.org/anthology/D19-1371>.

- [82] Arman Cohan, Sergey Feldman, Iz Beltagy, Doug Downey, and Daniel Weld. Specter: Document-level representation learning using citation-informed transformers. *ACL*, 2020.
- [83] Arman Cohan, Sergey Feldman, Iz Beltagy, Doug Downey, and Daniel S Weld. allenai-specter. <https://huggingface.co/sentence-transformers/allenai-specter>, 2020.
- [84] Recobo AI. Chemicalbert: Pretrained transformers for chemistry. <https://huggingface.co/recobo/chemical-bert-uncased>, 2023.
- [85] Nils Reimers and Iryna Gurevych. paraphrase-multilingual-mpnet-base-v2. <https://huggingface.co/sentence-transformers/paraphrase-multilingual-mpnet-base-v2>, 2021.
- [86] OpenAI. New embedding models and api updates. Technical report, OpenAI, 2024. URL <https://openai.com/index/new-embedding-models-and-api-updates/>. Accessed: 2025-05-19.
- [87] Hongliu Cao. Recent advances in text embedding: A comprehensive review of top-performing methods on the mteb benchmark. *arXiv preprint arXiv:2406.01607*, 2024.
- [88] Marti A Hearst. Multi-paragraph segmentation of expository text. *arXiv preprint cmp-lg/9406037*, 1994.
- [89] Freddy Choi. Linear text segmentation: approaches, advances and applications. *Proc. of CLUK3*, 2000.
- [90] Masao Utiyama and Hitoshi Isahara. A statistical model for domain-independent text segmentation. In *Proceedings of the 39th annual meeting of the Association for Computational Linguistics*, pages 499–506, 2001.
- [91] Regina Barzilay and Mirella Lapata. Modeling local coherence: An entity-based approach. *Computational Linguistics*, 34(1):1–34, 2008.
- [92] Hemant Misra, Franccois Yvon, Olivier Cappe, and Joemon Jose. Text segmentation: A topic modeling perspective. *Information Processing & Management*, 47(4):528–544, 2011.
- [93] Martin Riedl and Chris Biemann. Text segmentation with topic models. *Journal for Language Technology and Computational Linguistics*, 27(1):47–69, 2012.
- [94] Goran Glavavs, Federico Nanni, and Simone Paolo Ponzetto. Unsupervised text segmentation using semantic relatedness graphs. In *Proceedings of the Fifth Joint Conference on*

- Lexical and Computational Semantics*, pages 125–130. Association for Computational Linguistics, 2016.
- [95] Alessandro Solbiati, Kevin Heffernan, Georgios Damaskinos, Shivani Poddar, Shubham Modi, and Jacques Cali. Unsupervised topic segmentation of meetings with bert embeddings. *arXiv preprint arXiv:2106.12978*, 2021.
- [96] Yaxin Fan, Feng Jiang, Peifeng Li, and Haizhou Li. Uncovering the potential of chatgpt for discourse analysis in dialogue: An empirical study. *arXiv preprint arXiv:2305.08391*, 2023.
- [97] Junfeng Jiang, Chengzhang Dong, Sadao Kurohashi, and Akiko Aizawa. Superdialseg: A large-scale dataset for supervised dialogue segmentation. *arXiv preprint arXiv:2305.08371*, 2023.
- [98] Omri Koshorek, Adir Cohen, Noam Mor, Michael Rotman, and Jonathan Berant. Text segmentation as a supervised learning task. *arXiv preprint arXiv:1803.09337*, 2018.
- [99] Michal Lukasik, Boris Dadachev, Gonccalo Simoes, and Kishore Papineni. Text segmentation by cross segment attention. *arXiv preprint arXiv:2004.14535*, 2020.
- [100] Hai Yu, Chong Deng, Qinglin Zhang, Jiaqing Liu, Qian Chen, and Wen Wang. Improving long document topic segmentation models with enhanced coherence modeling. *arXiv preprint arXiv:2310.11772*, 2023.
- [101] Kelvin Lo, Yuan Jin, Weicong Tan, Ming Liu, Lan Du, and Wray Buntine. Transformer over pre-trained transformer for neural text segmentation with enhanced topic coherence. *arXiv preprint arXiv:2110.07160*, 2021.
- [102] Joe Barrow, Rajiv Jain, Vlad Morariu, Varun Manjunatha, Douglas W Oard, and Philip Resnik. A joint model for document segmentation and segment labeling. In *Proceedings of the 58th Annual Meeting of the Association for Computational Linguistics*, pages 313–322, 2020.
- [103] Swapna Somasundaran et al. Two-level transformer and auxiliary coherence modeling for improved text segmentation. In *Proceedings of the AAAI Conference on Artificial Intelligence*, volume 34, pages 7797–7804, 2020.
- [104] Zheng Gong, Shiwei Tong, Han Wu, Qi Liu, Hanqing Tao, Wei Huang, and Runlong Yu. Tipster: A topic-guided language model for topic-aware text segmentation. In *International Conference on Database Systems for Advanced Applications*, pages 213–221. Springer, 2022.

- [105] Iacopo Ghinassi, Lin Wang, Chris Newell, and Matthew Purver. Recent trends in linear text segmentation: A survey. *arXiv preprint arXiv:2411.16613*, 2024.
- [106] Alina Petukhova, Joao P Matos-Carvalho, and Nuno Fachada. Text clustering with llm embeddings. *arXiv e-prints*, pages arXiv–2403, 2024.
- [107] Tomas Mikolov, Kai Chen, Greg Corrado, and Jeffrey Dean. Efficient estimation of word representations in vector space. *arXiv preprint arXiv:1301.3781*, 2013.
- [108] Jeffrey Pennington, Richard Socher, and Christopher D Manning. Glove: Global vectors for word representation. In *Proceedings of the 2014 conference on empirical methods in natural language processing (EMNLP)*, pages 1532–1543, 2014.
- [109] Piotr Bojanowski, Edouard Grave, Armand Joulin, and Tomas Mikolov. Enriching word vectors with subword information. *Transactions of the association for computational linguistics*, 5:135–146, 2017.
- [110] Hritvik Gupta and Mayank Patel. Study of extractive text summarizer using the elmo embedding. In *2020 Fourth International Conference on I-SMAC (IoT in Social, Mobile, Analytics and Cloud)(I-SMAC)*, pages 829–834. IEEE, 2020.
- [111] Jacob Devlin, Ming-Wei Chang, Kenton Lee, and Kristina Toutanova. Bert: Pre-training of deep bidirectional transformers for language understanding. In *Proceedings of the 2019 conference of the North American chapter of the association for computational linguistics: human language technologies, volume 1 (long and short papers)*, pages 4171–4186, 2019.
- [112] Alec Radford, Karthik Narasimhan, Tim Salimans, Ilya Sutskever, et al. Improving language understanding by generative pre-training. 2018.
- [113] Zehan Li, Xin Zhang, Yanzhao Zhang, Dingkun Long, Pengjun Xie, and Meishan Zhang. Towards general text embeddings with multi-stage contrastive learning. *arXiv preprint arXiv:2308.03281*, 2023.
- [114] Shitao Xiao, Zheng Liu, Peitian Zhang, Niklas Muennighoff, Defu Lian, and Jian-Yun Nie. C-pack: Packed resources for general chinese embeddings. In *Proceedings of the 47th international ACM SIGIR conference on research and development in information retrieval*, pages 641–649, 2024.
- [115] Nils Reimers and Iryna Gurevych. Sentence-transformers. <https://www.sbert.net>, 2019.
- [116] Yu Gu, Robert Tinn, Hao Cheng, Michael Lucas, Naoto Usuyama, Xiaodong Liu, Tristan Naumann, Jianfeng Gao, and Hoifung Poon. Domain-specific language model

- pretraining for biomedical natural language processing, 2020. Available at <https://arxiv.org/abs/2007.15779>.
- [117] Souradip Chakraborty, Ekaba Bisong, Shweta Bhatt, Thomas Wagner, Riley Elliott, and Francesco Mosconi. Biomedbert: A pre-trained biomedical language model for qa and ir, 2020. URL <https://aclanthology.org/2020.coling-main.59/>.
- [118] Recobo. Chemicalbert: A bert model for the chemical domain, 2021. Available at <https://huggingface.co/recobo/chemical-bert-uncased>.
- [119] Tanishq Gupta, Mohd Zaki, N. M. Anoop Krishnan, and Mausam. Matscibert: A materials domain language model for text mining and information extraction. *npj Computational Materials*, 8(1):102, 2022. doi: 10.1038/s41524-022-00784-w. URL <https://www.nature.com/articles/s41524-022-00784-w>.
- [120] Zach Nussbaum, John X. Morris, Brandon Duderstadt, and Andriy Mulyar. Training sparse mixture of experts text embedding models. *arXiv preprint arXiv:2502.07972*, 2024. URL <https://arxiv.org/abs/2502.07972>.
- [121] Saba Sturua, Isabelle Mohr, Mohammad Kalim Akram, Michael Gunther, Bo Wang, Markus Krimmel, Feng Wang, Georgios Mastrapas, Andreas Koukounas, Nan Wang, and Han Xiao. Jina embeddings v3: Multilingual embeddings with task lora. *arXiv preprint arXiv:2409.10173*, 2024. URL <https://arxiv.org/abs/2409.10173>.
- [122] Liang Wang, Nan Yang, Xiaolong Huang, Linjun Yang, Rangan Majumder, and Furu Wei. Multilingual e5 text embeddings: A technical report. *arXiv preprint arXiv:2402.05672*, 2024. URL <https://arxiv.org/abs/2402.05672>.
- [123] Yiming Xu, Yuxuan Liu, Yichang Zhang, Xinyu Wang, Ziyang Liu, Yiming Wang, Yujie Wang, Yuxuan Wang, Xiangyang Zhang, Zhiyuan Liu, et al. Bge m3-embedding: Multi-lingual, multi-functionality, multi-granularity embedding model. *arXiv preprint arXiv:2402.03216*, 2024. URL <https://arxiv.org/abs/2402.03216>.

7 Supplementary Materials

7.1 Related Work on Chunking Strategies

Linear Text Segmentation (LTS), or topic segmentation, involves detecting boundaries in text where topical shifts occur. This structural understanding is essential for a variety of downstream NLP tasks such as summarization, information retrieval, and document classification.

Despite a wealth of research in general-purpose segmentation[105], domain-specific applications—particularly in scientific disciplines such as chemistry—are still underexplored.

Unsupervised methods have traditionally dominated early segmentation efforts. TextTiling [88] used lexical cohesion between sentence windows to detect topic changes. C99 [89] improved on this by applying divisive clustering, while U00 [90] introduced a dynamic programming framework. BayesSeg [91] advanced these methods with probabilistic cue phrase modeling.

Topic modeling methods, such as those based on Latent Dirichlet Allocation (LDA), inferred latent topic distributions and aligned segments accordingly [92, 93]. These generative approaches allow hierarchical and probabilistic interpretations of segment structure, which align well with the nested topics in scientific texts.

With the rise of contextual word and sentence embeddings, embedding-based methods became more prominent. GraphSeg [94] and BERT-based adaptations [95] demonstrated how dense vector similarity between sentences can yield more semantically grounded segmentation. Transformer-based encoders like BERT and Longformer have further enhanced the modeling of coherence and topic boundaries.

Large Language Models (LLMs) such as ChatGPT have recently been used in zero-shot settings to segment text through prompt engineering. Studies by Fan and Jiang [96] and Jiang et al. [97] show that LLMs can outperform many traditional methods on dialogue segmentation, with promising implications for low-resource domains like scientific literature.

Supervised segmentation approaches have evolved significantly due to the advent of pre-trained transformers. TextSeg [98] framed segmentation as a binary sequence tagging task. Later systems like Cross-Segment BERT [99] and Longformer + TSSP + CSSL [100] utilized contextual embeddings to model sentence transitions more accurately.

However, these supervised systems often overfit to domain-specific patterns, limiting their generalizability. To address this, multi-task learning approaches combine segmentation with auxiliary tasks like topic classification or coherence modeling [101–103]. These systems learn shared representations that focus on thematic coherence rather than surface cues. For instance, Tipster [104] integrates neural topic modeling with segmentation, guiding BERT-based sentence embeddings with topic distributions.

Coherence-aware losses have also been introduced, penalizing incoherence within topic segments by leveraging contrastive learning or corrupted input detection. These models have shown improved robustness across datasets and better semantic alignment of segments.

Retrieval-Augmented Generation (RAG) systems combine external knowledge retrieval with generation. The input to the retriever typically consists of segmented text chunks. Thus, the granularity and coherence of segmentation directly impact retrieval precision and the quality of generated responses.

Poor segmentation can result in retrieving irrelevant or incomplete text spans, especially harmful in technical domains like chemistry where precision is crucial. For example, sepa-

rating a definition from its context or a method from its findings may lead to factual errors in generation.

Furthermore, most segmentation models have been developed for general-purpose or Wikipedia-style content. Scientific texts differ significantly in structure, terminology, and topic granularity. This gap motivates the need for domain-adapted segmentation models specifically evaluated for RAG performance.

Although recent work has demonstrated strong performance from supervised and LLM-based segmentation models, applications to the chemistry domain remain rare. Annotated datasets in chemistry are scarce, and few methods have been adapted or evaluated on such data. While some unsupervised methods (e.g., BayesSeg, ChatGPT zero-shot segmentation) offer generalizability, they have not been tested against the structural and semantic complexity of chemical texts.

7.2 Related Work on Embedding Models

The representation of textual data through embeddings has undergone a significant transformation, fundamentally reshaping how machines interpret and utilize human language. This evolution can be broadly divided into four eras, each characterized by increasingly sophisticated approaches to capturing semantic meaning[87].

The first era centered on count-based methods, such as Bag-of-Words (BoW) and Term Frequency–Inverse Document Frequency (TF-IDF)[106]. These techniques encoded text as sparse, high-dimensional vectors, offering utility in basic term matching but failing to account for semantic similarity or contextual nuance.

The second era introduced static word embeddings, marking a shift towards distributed representations. Models like Word2Vec[107], GloVe[108], and FastText[109] embedded words into dense vector spaces based on their co-occurrence in large corpora. While effective in capturing analogical relationships and general semantics, these models were context-invariant, assigning a single vector per word irrespective of usage.

The third era was defined by the emergence of contextualized embeddings through deep neural architectures. ELMo[110], BERT[111], and GPT[112] generated dynamic token embeddings conditioned on surrounding context, greatly enhancing performance across a broad range of NLP tasks. However, these models often required task-specific fine-tuning and imposed substantial computational demands.

The field has now entered the fourth era, characterized by universal embedding models—general-purpose encoders that produce robust semantic representations applicable across tasks and domains without additional fine-tuning. Models such as E5[42], GTE[113], and BGE [114] exemplify this paradigm, delivering high-quality embeddings suitable for information retrieval, clustering, classification, and ranking. These models are particularly well-suited for Retrieval-Augmented Generation (RAG) frameworks, where efficient and accurate retrieval is essential

to grounding the outputs of generative models.

In RAG systems, the embedding model underpins the retriever’s ability to map user queries and candidate documents into a shared vector space for semantic similarity search. This process is especially critical in the chemistry domain, where textual data contains complex entities, specialized terminology, and high demands for factual accuracy. Consequently, embedding models must balance semantic generalization with domain-specific sensitivity to ensure relevant and precise retrieval.

Early implementations in this space often relied on Sentence-BERT (SBERT)[23], which adapted BERT[111] using a Siamese or triplet architecture to generate sentence-level embeddings optimized for similarity tasks. Variants such as bert-base-nli-mean-tokens⁸[111], all-MiniLM-L6-v2⁹[38], all-mpnet-base-v2¹⁰[40], and multi-qa-mpnet-base-dot-v1¹¹[40] offer practical trade-offs between performance and efficiency. Despite their strong general-domain performance, these models frequently underperform in scientific contexts due to their lack of exposure to technical language.

Recent progress has focused on instruction-tuned embeddings, designed to align model outputs with real-world intents such as querying, ranking, and paraphrasing. The E5[42] family, trained on large-scale contrastive learning datasets like Colossal Clean Pairs (CCPairs), and the BGE[114] series, which incorporate in-batch negatives and synthetic QA data, demonstrate strong zero-shot performance across retrieval benchmarks. Notably, multitask variants such as bge-m3¹²[59] further enhance performance by jointly optimizing for retrieval, classification, and semantic similarity.

To address the challenges of scientific retrieval, several domain-specific embedding models have been developed. For instance, SciBERT[80] is trained on scientific literature and has shown consistent improvements in academic NLP tasks. Biomedical-focused models such as PubMedBERT[116] and BiomedBERT[117] capture terminology relevant to pharmacology and toxicology. In the chemistry subdomain, ChemicalBERT (recobo)[118], ChemBERTa (DeepChem)[69], and MatSciBERT (m3rg-iitd)[119] offer embeddings tailored to chemical compounds, reactions, and material science literature, outperforming generalist models in retrieval tasks that demand domain precision.

Finally, multilingual and instruction-tuned models such as Nomic Embed[120], Jina Embeddings[121], and multilingual variants of BGE and E5 (e.g., multilingual-e5[122], bge-multilingual[123]) are gaining traction for applications involving non-English chemical patents, safety documents, and global scientific publications.

This study systematically evaluates the impact of embedding models—ranging from general-purpose to domain-specific—on the performance of RAG systems within the chemistry domain.

⁸<https://huggingface.co/sentence-transformers/bert-base-nli-mean-tokens>

⁹<https://huggingface.co/sentence-transformers/all-MiniLM-L6-v2>

¹⁰<https://huggingface.co/sentence-transformers/all-mpnet-base-v2>

¹¹<https://huggingface.co/sentence-transformers/multi-qa-mpnet-base-dot-v1>

¹²<https://huggingface.co/BAAI/bge-m3>

We analyze the trade-offs between universality and specialization, and assess how emerging models, particularly instruction-tuned and multitask embeddings, enhance document retrieval precision and downstream generative accuracy. Our results inform the development of RAG systems tailored for scientific applications, where both semantic understanding and factual reliability are paramount.

7.3 Supplementary Tables: Detailed Evaluation of Chunking Strategies and Embedding Models

This section provides the original tabular results supporting the main experiments presented in the paper. It includes detailed performance metrics for various chunking strategies and embedding models across chemistry-specific retrieval tasks. Tables report standard IR metrics (e.g., IoU, Recall, Precision, F2, NDCG@10, MAP@10) under different configurations, and are organized to support reproducibility, comparison, and further analysis beyond the visual summaries provided in the main text.

Table 7: Comparison of chunking methods across various configurations, including chunk size and overlap, in a retrieval-augmented generation (RAG) system for chemistry. Metrics include mean and standard deviation for Intersection over Union (IoU), Recall, and Precision at threshold Ω .

Method	Chunk Size	Overlap Size	IoU	Recall	Precision@ Ω	Precision
CL	NaN	NaN	0.030 \pm 0.024	0.709 \pm 0.438	0.174 \pm 0.091	0.031 \pm 0.024
FX128-25	128.000000	25.000000	0.053 \pm 0.040	0.709 \pm 0.429	0.246 \pm 0.094	0.054 \pm 0.040
FX256-50	256.000000	50.000000	0.027 \pm 0.021	0.701 \pm 0.447	0.146 \pm 0.066	0.027 \pm 0.021
FX512-100	512.000000	100.000000	0.013 \pm 0.011	0.675 \pm 0.463	0.079 \pm 0.035	0.013 \pm 0.011
FX64-12	64.000000	12.000000	0.092 \pm 0.069	0.648 \pm 0.420	0.377 \pm 0.106	0.094 \pm 0.070
KM100	100.000000	0.000000	0.039 \pm 0.037	0.693 \pm 0.437	0.219 \pm 0.141	0.039 \pm 0.038
KM200	200.000000	0.000000	0.019 \pm 0.020	0.659 \pm 0.464	0.119 \pm 0.095	0.019 \pm 0.020
KM400	400.000000	0.000000	0.011 \pm 0.012	0.663 \pm 0.470	0.065 \pm 0.063	0.011 \pm 0.012
KM50	50.000000	0.000000	0.083 \pm 0.072	0.639 \pm 0.424	0.375 \pm 0.159	0.085 \pm 0.073
LLM	NaN	NaN	0.024 \pm 0.019	0.721 \pm 0.443	0.140 \pm 0.085	0.024 \pm 0.019
RT100-20	100.000000	20.000000	0.090 \pm 0.066	0.707 \pm 0.413	0.357 \pm 0.142	0.091 \pm 0.067
RT128-32	128.000000	32.000000	0.071 \pm 0.053	0.717 \pm 0.420	0.300 \pm 0.130	0.071 \pm 0.054
RT256-64	256.000000	64.000000	0.038 \pm 0.029	0.719 \pm 0.435	0.196 \pm 0.098	0.038 \pm 0.029
RT512-128	512.000000	128.000000	0.018 \pm 0.015	0.683 \pm 0.462	0.108 \pm 0.053	0.018 \pm 0.015
RT64-16	64.000000	16.000000	0.123 \pm 0.093	0.638 \pm 0.413	0.432 \pm 0.147	0.126 \pm 0.095

Table 11: Performance summary of the top embedding models across individual chemistry retrieval tasks. Each row presents a model’s average score on one task, using six standard IR metrics: Main Score, NDCG@10, MAP@10, Recall@10, Precision@10, and MRR@10. Short model names are used for compact presentation.

Short Model	Task	Main Score	MAP@10	MRR@10	NDCG@10	Precision@10	Recall@10
AI_SciBERT	ChemHotpotQARetrieval	0.351300	0.319400	0.319400	0.351300	0.044400	0.444400
AI_SciBERT	ChemNQRetrieval	0.044600	0.039700	0.042300	0.044600	0.007400	0.055600
AI_SciBERT	FSUChemRxivQest	0.129300	0.092500	0.139600	0.129300	0.030600	0.192200
AI_Specter	ChemHotpotQARetrieval	0.324200	0.286100	0.286100	0.324200	0.044400	0.444400

Continued on next page

Table 11 (continued): Performance summary of the top embedding models (continued).

Short Model	Task	Main Score	MAP@10	MRR@10	NDCG@10	Precision@10	Recall@10
AI_Specter	ChemNQRetrieval	0.118000	0.071600	0.085500	0.118000	0.033300	0.240700
AI_Specter	FSUChemRxivQest	0.211100	0.159200	0.229600	0.211100	0.046100	0.295400
BAAI_bgeB	ChemHotpotQARetrieval	0.803600	0.776500	0.776500	0.803600	0.088900	0.888900
BAAI_bgeB	ChemNQRetrieval	0.589200	0.513100	0.555200	0.589200	0.100000	0.765400
BAAI_bgeB	FSUChemRxivQest	0.484900	0.397600	0.524300	0.484900	0.092700	0.618300
BAAI_bgeB_v1.5	ChemHotpotQARetrieval	0.812800	0.805600	0.805600	0.812800	0.083300	0.833300
BAAI_bgeB_v1.5	ChemNQRetrieval	0.611800	0.525400	0.546400	0.611800	0.111100	0.839500
BAAI_bgeB_v1.5	FSUChemRxivQest	0.490800	0.402800	0.532000	0.490800	0.093400	0.625500
BAAI_bgeL	ChemHotpotQARetrieval	0.797800	0.768500	0.768500	0.797800	0.088900	0.888900
BAAI_bgeL	ChemNQRetrieval	0.557200	0.451000	0.496400	0.557200	0.107400	0.839500
BAAI_bgeL	FSUChemRxivQest	0.493000	0.406100	0.540200	0.493000	0.092800	0.618400
BAAI_bgeL_v1.5	ChemHotpotQARetrieval	0.817600	0.777800	0.777800	0.817600	0.094400	0.944400
BAAI_bgeL_v1.5	ChemNQRetrieval	0.599000	0.513400	0.549200	0.599000	0.103700	0.827200
BAAI_bgeL_v1.5	FSUChemRxivQest	0.491600	0.404400	0.536600	0.491600	0.093200	0.620500
BAAI_bgeM3	ChemHotpotQARetrieval	0.773900	0.736100	0.736100	0.773900	0.088900	0.888900
BAAI_bgeM3	ChemNQRetrieval	0.589600	0.503200	0.538300	0.589600	0.103700	0.802500
BAAI_bgeM3	FSUChemRxivQest	0.505900	0.418200	0.555800	0.505900	0.094500	0.632300
BAAI_bgeS	ChemHotpotQARetrieval	0.746400	0.700900	0.700900	0.746400	0.088900	0.888900
BAAI_bgeS	ChemNQRetrieval	0.293000	0.209000	0.243200	0.293000	0.066700	0.512400
BAAI_bgeS_v1.5	ChemHotpotQARetrieval	0.785300	0.737100	0.737100	0.785300	0.094400	0.944400
BAAI_bgeS_v1.5	ChemNQRetrieval	0.499200	0.395900	0.455000	0.499200	0.096300	0.746900
BAAI_bgeS_v1.5	FSUChemRxivQest	0.471800	0.387200	0.512800	0.471800	0.089600	0.599600
DC_ChemBERTa	ChemHotpotQARetrieval	0.016700	0.006200	0.006200	0.016700	0.005600	0.055600
DC_ChemBERTa	ChemNQRetrieval	0.000000	0.000000	0.000000	0.000000	0.000000	0.000000
DC_ChemBERTa	FSUChemRxivQest	0.000000	0.000000	0.000000	0.000000	0.000000	0.000000
Desc_Gemini	ChemHotpotQARetrieval	0.257300	0.231500	0.231500	0.257300	0.033300	0.333300
Desc_Gemini	ChemNQRetrieval	0.114900	0.084900	0.112700	0.114900	0.022200	0.185200
Desc_Gemini	FSUChemRxivQest	0.140900	0.105800	0.158800	0.140900	0.030000	0.193600
FB_contriever	ChemHotpotQARetrieval	0.598000	0.577400	0.577400	0.598000	0.066700	0.666700
FB_contriever	ChemNQRetrieval	0.350600	0.299700	0.349400	0.350600	0.055600	0.463000
FB_contriever	FSUChemRxivQest	0.322900	0.244200	0.334200	0.322900	0.070800	0.466700
FB_contrieverMS	ChemHotpotQARetrieval	0.708300	0.666700	0.666700	0.708300	0.083300	0.833300
FB_contrieverMS	ChemNQRetrieval	0.496300	0.416700	0.451200	0.496300	0.092600	0.697500
FB_contrieverMS	FSUChemRxivQest	0.474100	0.388200	0.515500	0.474100	0.090700	0.604500
GGL_BERTbU	ChemHotpotQARetrieval	0.423900	0.416700	0.416700	0.423900	0.044400	0.444400
GGL_BERTbU	ChemNQRetrieval	0.141300	0.107200	0.147500	0.141300	0.029600	0.203700
HKU_InstructXL	ChemHotpotQARetrieval	0.742000	0.731500	0.731500	0.742000	0.077800	0.777800
HKU_InstructXL	ChemNQRetrieval	0.575600	0.465500	0.507500	0.575600	0.107400	0.864200
HKU_InstructXL	FSUChemRxivQest	0.491600	0.403900	0.537100	0.491600	0.092900	0.622000
IITD_MatSci	ChemHotpotQARetrieval	0.218400	0.199100	0.199100	0.218400	0.027800	0.277800
IITD_MatSci	ChemNQRetrieval	0.000000	0.000000	0.000000	0.000000	0.000000	0.000000
IITD_MatSci	FSUChemRxivQest	0.106400	0.076900	0.114400	0.106400	0.024100	0.158100
Intf_e5B	ChemHotpotQARetrieval	0.785000	0.768500	0.768500	0.785000	0.083300	0.833300
Intf_e5B	ChemNQRetrieval	0.622000	0.523900	0.554600	0.622000	0.114800	0.876500
Intf_e5B	FSUChemRxivQest	0.518000	0.426900	0.566800	0.518000	0.097600	0.650700
Intf_e5B_v2	ChemHotpotQARetrieval	0.738300	0.727800	0.727800	0.738300	0.077800	0.777800
Intf_e5B_v2	ChemNQRetrieval	0.620500	0.520800	0.568400	0.620500	0.114800	0.876500
Intf_e5B_v2	FSUChemRxivQest	0.498700	0.408100	0.541300	0.498700	0.095600	0.636800
Intf_e5L	ChemHotpotQARetrieval	0.785000	0.768500	0.768500	0.785000	0.083300	0.833300
Intf_e5L	ChemNQRetrieval	0.608500	0.503000	0.543300	0.608500	0.114800	0.876500
Intf_e5L	FSUChemRxivQest	0.522400	0.434500	0.572000	0.522400	0.097000	0.648100
Intf_e5L_v2	ChemHotpotQARetrieval	0.757300	0.750000	0.750000	0.757300	0.077800	0.777800
Intf_e5L_v2	ChemNQRetrieval	0.694400	0.610600	0.650700	0.694400	0.114800	0.901200

Continued on next page

Table 11 (continued): Performance summary of the top embedding models (continued).

Short Model	Task	Main Score	MAP@10	MRR@10	NDCG@10	Precision@10	Recall@10
Intf_e5L_v2	FSUChemRxivQest	0.523300	0.434000	0.574400	0.523300	0.098000	0.650400
Intf_e5S	ChemHotpotQARetrieval	0.781300	0.746900	0.746900	0.781300	0.088900	0.888900
Intf_e5S	ChemNQRetrieval	0.592000	0.491400	0.553700	0.592000	0.107400	0.827200
Intf_e5S	FSUChemRxivQest	0.500100	0.412800	0.548300	0.500100	0.093500	0.625300
Intf_e5S_v2	ChemHotpotQARetrieval	0.743700	0.733300	0.733300	0.743700	0.077800	0.777800
Intf_e5S_v2	ChemNQRetrieval	0.637800	0.553500	0.602200	0.637800	0.111100	0.839500
Intf_e5S_v2	FSUChemRxivQest	0.502800	0.414800	0.556500	0.502800	0.093900	0.624400
Intf_mE5B	ChemHotpotQARetrieval	0.701700	0.675900	0.675900	0.701700	0.077800	0.777800
Intf_mE5B	ChemNQRetrieval	0.650700	0.542300	0.591700	0.650700	0.118500	0.913600
Intf_mE5B	FSUChemRxivQest	0.509300	0.422200	0.560800	0.509300	0.095400	0.632000
Intf_mE5L	ChemHotpotQARetrieval	0.684300	0.654600	0.654600	0.684300	0.077800	0.777800
Intf_mE5L	ChemNQRetrieval	0.661700	0.563400	0.583300	0.661700	0.118500	0.913600
Intf_mE5L	FSUChemRxivQest	0.517600	0.428400	0.572700	0.517600	0.096400	0.641400
Intf_mE5S	ChemHotpotQARetrieval	0.823300	0.785800	0.785800	0.823300	0.094400	0.944400
Intf_mE5S	ChemNQRetrieval	0.704600	0.633400	0.706800	0.704600	0.107400	0.845700
Intf_mE5S	FSUChemRxivQest	0.485400	0.397900	0.534700	0.485400	0.091400	0.612100
Jina_v2B	ChemHotpotQARetrieval	0.000000	0.000000	0.000000	0.000000	0.000000	0.000000
Jina_v2B	ChemNQRetrieval	0.000000	0.000000	0.000000	0.000000	0.000000	0.000000
Jina_v2S	ChemHotpotQARetrieval	0.129600	0.119000	0.119000	0.129600	0.016700	0.166700
Jina_v2S	ChemNQRetrieval	0.000000	0.000000	0.000000	0.000000	0.000000	0.000000
MQA_MPNetB	ChemHotpotQARetrieval	0.604800	0.566700	0.566700	0.604800	0.072200	0.722200
MQA_MPNetB	ChemNQRetrieval	0.531800	0.426200	0.497700	0.531800	0.103700	0.784000
MS_BiomedBERT_a	ChemHotpotQARetrieval	0.271800	0.250000	0.250000	0.271800	0.033300	0.333300
MS_BiomedBERT_a	ChemNQRetrieval	0.140300	0.103700	0.120200	0.140300	0.029600	0.240700
MS_BiomedBERT_a	FSUChemRxivQest	0.186300	0.142000	0.203100	0.186300	0.039000	0.258000
MS_MPNetB	ChemHotpotQARetrieval	0.229500	0.213000	0.213000	0.229500	0.027800	0.277800
MS_MPNetB	ChemNQRetrieval	0.058900	0.047100	0.049700	0.058900	0.011100	0.092600
MS_MPNetB	FSUChemRxivQest	0.120000	0.092200	0.133000	0.120000	0.024600	0.163400
MS_MiniLM384	ChemHotpotQARetrieval	0.017500	0.006900	0.006900	0.017500	0.005600	0.055600
MS_MiniLM384	ChemNQRetrieval	0.000000	0.000000	0.000000	0.000000	0.000000	0.000000
MS_MiniLM384	FSUChemRxivQest	0.009100	0.006200	0.012100	0.009100	0.002200	0.011700
MS_PubMedBERT_a	ChemHotpotQARetrieval	0.271800	0.250000	0.250000	0.271800	0.033300	0.333300
MS_PubMedBERT_a	ChemNQRetrieval	0.140300	0.103700	0.120200	0.140300	0.029600	0.240700
MS_PubMedBERT_a	FSUChemRxivQest	0.186300	0.142000	0.203100	0.186300	0.039000	0.258000
MS_PubMedBERT_af	ChemHotpotQARetrieval	0.324400	0.272800	0.272800	0.324400	0.050000	0.500000
MS_PubMedBERT_af	ChemNQRetrieval	0.115300	0.096300	0.118500	0.115300	0.018500	0.148200
MS_PubMedBERT_af	FSUChemRxivQest	0.214600	0.164000	0.229800	0.214600	0.045300	0.300000
Nomic_BERT2048	ChemHotpotQARetrieval	0.073100	0.062500	0.062500	0.073100	0.011100	0.111100
Nomic_BERT2048	ChemNQRetrieval	0.026000	0.013900	0.023100	0.026000	0.007400	0.055600
Nomic_text_v1	ChemHotpotQARetrieval	0.871800	0.847200	0.847200	0.871800	0.094400	0.944400
Nomic_text_v1	ChemNQRetrieval	0.649200	0.558600	0.609600	0.649200	0.114800	0.870400
Nomic_text_v1	FSUChemRxivQest	0.516400	0.427400	0.567000	0.516400	0.096600	0.643800
Nomic_text_v1.5	ChemHotpotQARetrieval	0.854800	0.825900	0.825900	0.854800	0.094400	0.944400
Nomic_text_v1.5	ChemNQRetrieval	0.637400	0.528900	0.568500	0.637400	0.122200	0.925900
Nomic_text_v1.5	FSUChemRxivQest	0.492900	0.408200	0.539600	0.492900	0.092000	0.616400
Rec_ChemBERT	ChemHotpotQARetrieval	0.223700	0.188500	0.188500	0.223700	0.033300	0.333300
Rec_ChemBERT	ChemNQRetrieval	0.125700	0.100300	0.132700	0.125700	0.022200	0.166700
Rec_ChemBERT	FSUChemRxivQest	0.169800	0.129800	0.186700	0.169800	0.035100	0.233400
Sent_BERTnli	ChemHotpotQARetrieval	0.309000	0.284000	0.284000	0.309000	0.038900	0.388900
Sent_BERTnli	ChemNQRetrieval	0.212700	0.185200	0.203700	0.212700	0.033300	0.277800
Sent_BERTnli	FSUChemRxivQest	0.075100	0.059100	0.079400	0.075100	0.014500	0.102500
Sent_MQA_MPNetB	ChemHotpotQARetrieval	0.604800	0.566700	0.566700	0.604800	0.072200	0.722200
Sent_MQA_MPNetB	ChemNQRetrieval	0.531800	0.426200	0.497700	0.531800	0.103700	0.784000

Continued on next page

Table 11 (continued): Performance summary of the top embedding models (continued).

Short Model	Task	Main Score	MAP@10	MRR@10	NDCG@10	Precision@10	Recall@10
Sent_MQA_MPNNetB	FSUChemRxivQest	0.466800	0.382000	0.509600	0.466800	0.088400	0.593900
Sent_MiniLM12_v2	ChemHotpotQARetrieval	0.598500	0.559300	0.559300	0.598500	0.072200	0.722200
Sent_MiniLM12_v2	ChemNQRetrieval	0.570000	0.485500	0.530600	0.570000	0.100000	0.784000
Sent_MiniLM12_v2	FSUChemRxivQest	0.391300	0.311300	0.414600	0.391300	0.079400	0.526100
Sent_MiniLM6_v2	ChemHotpotQARetrieval	0.675900	0.645500	0.645500	0.675900	0.077800	0.777800
Sent_MiniLM6_v2	ChemNQRetrieval	0.549400	0.450700	0.501100	0.549400	0.103700	0.808600
Sent_MiniLM6_v2	FSUChemRxivQest	0.403600	0.326000	0.433800	0.403600	0.079300	0.527600
Sent_allMPNetB_v2	ChemHotpotQARetrieval	0.586800	0.561700	0.561700	0.586800	0.066700	0.666700
Sent_allMPNetB_v2	ChemNQRetrieval	0.529500	0.444700	0.472100	0.529500	0.096300	0.746900
Sent_allMPNetB_v2	FSUChemRxivQest	0.364100	0.290600	0.386300	0.364100	0.074700	0.487800
Sent_gtrT5_B	ChemHotpotQARetrieval	0.538200	0.517300	0.517300	0.538200	0.061100	0.611100
Sent_gtrT5_B	ChemNQRetrieval	0.566300	0.463400	0.522400	0.566300	0.103700	0.827200
Sent_gtrT5_B	FSUChemRxivQest	0.456700	0.372600	0.497400	0.456700	0.087000	0.583300
Sent_gtrT5_L	ChemHotpotQARetrieval	0.576700	0.531200	0.531200	0.576700	0.072200	0.722200
Sent_gtrT5_L	ChemNQRetrieval	0.545400	0.450200	0.480700	0.545400	0.103700	0.808600
Sent_gtrT5_L	FSUChemRxivQest	0.477300	0.390200	0.522600	0.477300	0.090400	0.605400
Sent_gtrT5_XL	ChemHotpotQARetrieval	0.635100	0.608000	0.608000	0.635100	0.072200	0.722200
Sent_gtrT5_XL	ChemNQRetrieval	0.543800	0.429400	0.473500	0.543800	0.107400	0.839500
Sent_gtrT5_XL	FSUChemRxivQest	0.477600	0.392800	0.526300	0.477600	0.089200	0.599200
Sent_paraMPNetB_v2	ChemHotpotQARetrieval	0.524300	0.479600	0.479600	0.524300	0.066700	0.666700
Sent_paraMPNetB_v2	ChemNQRetrieval	0.443500	0.357200	0.396300	0.443500	0.081500	0.666700
Sent_paraMPNetB_v2	FSUChemRxivQest	0.392100	0.315400	0.418800	0.392100	0.077200	0.517300

Table 12: Per-task performance of all evaluated models, showing each model’s best configuration in terms of F_2 score. Precision and recall at cutoff 10 are also reported to provide a breakdown of the F_2 components.

Task	Model	F_2	Precision@10	Recall@10
ChemHotpotQARetrieval	BAAI_bgeL_v1.5	0.3373	0.0944	0.9444
ChemHotpotQARetrieval	BAAI_bgeS_v1.5	0.3373	0.0944	0.9444
ChemHotpotQARetrieval	Intf_mE5S	0.3373	0.0944	0.9444
ChemHotpotQARetrieval	Nomic_text_v1	0.3373	0.0944	0.9444
ChemHotpotQARetrieval	Nomic_text_v1.5	0.3373	0.0944	0.9444
ChemHotpotQARetrieval	BAAI_bgeB	0.3175	0.0889	0.8889
ChemHotpotQARetrieval	BAAI_bgeL	0.3175	0.0889	0.8889
ChemHotpotQARetrieval	BAAI_bgeM3	0.3175	0.0889	0.8889
ChemHotpotQARetrieval	BAAI_bgeS	0.3175	0.0889	0.8889
ChemHotpotQARetrieval	Intf_e5S	0.3175	0.0889	0.8889
ChemNQRetrieval	Nomic_text_v1.5	0.3999	0.1222	0.9259
ChemNQRetrieval	Intf_mE5B	0.3901	0.1185	0.9136
ChemNQRetrieval	Intf_mE5L	0.3901	0.1185	0.9136
ChemNQRetrieval	Intf_e5L_v2	0.3803	0.1148	0.9012
ChemNQRetrieval	Intf_e5B	0.3767	0.1148	0.8765
ChemNQRetrieval	Intf_e5B_v2	0.3767	0.1148	0.8765
ChemNQRetrieval	Intf_e5L	0.3767	0.1148	0.8765
ChemNQRetrieval	Nomic_text_v1	0.3758	0.1148	0.8704
ChemNQRetrieval	BAAI_bgeB_v1.5	0.3633	0.1111	0.8395
ChemNQRetrieval	Intf_e5S_v2	0.3633	0.1111	0.8395
FSUChemRxivQest	Intf_e5L_v2	0.3058	0.0980	0.6504
FSUChemRxivQest	Intf_e5B	0.3051	0.0976	0.6507
FSUChemRxivQest	Intf_e5L	0.3034	0.0970	0.6481

Continued on next page

Table 12: Per-task performance of all evaluated models, showing each model’s best configuration in terms of F_2 score. Precision and recall at cutoff 10 are also reported to provide a breakdown of the F_2 components.

Task	Model	F_2	Precision@10	Recall@10
FSUChemRxivQest	Nomic_text_v1	0.3019	0.0966	0.6438
FSUChemRxivQest	Intf_mE5L	0.3010	0.0964	0.6414
FSUChemRxivQest	Intf_e5B_v2	0.2986	0.0956	0.6368
FSUChemRxivQest	Intf_mE5B	0.2974	0.0954	0.6320
FSUChemRxivQest	BAAI_bgeM3	0.2958	0.0945	0.6323
FSUChemRxivQest	Intf_e5S_v2	0.2932	0.0939	0.6244
FSUChemRxivQest	Intf_e5S	0.2925	0.0935	0.6253

Table 8: Precision and recall metrics (mean values) for each chunking method evaluated, sorted by F_2 score to emphasize performance with stronger recall weighting. Bubble sizes and colors in the related figure correspond to F_1 and F_2 scores respectively.

Method	Precision_mean	Recall_mean	F_1	F_2
RT100-20	0.090800	0.707100	0.161000	0.560700
RT64-16	0.126000	0.637800	0.210500	0.551700
RT128-32	0.071500	0.717100	0.130000	0.532200
FX64-12	0.093800	0.647600	0.163800	0.527700
KM50	0.084700	0.639300	0.149600	0.510600
FX128-25	0.053600	0.708900	0.099600	0.482100
RT256-64	0.037600	0.719100	0.071500	0.423700
KM100	0.039300	0.693300	0.074400	0.422800
CL	0.030500	0.709200	0.058500	0.382200
FX256-50	0.027100	0.700700	0.052100	0.358100
LLM	0.023900	0.721100	0.046300	0.339800
KM200	0.019400	0.659200	0.037600	0.290400
RT512-128	0.017600	0.682700	0.034300	0.278300
FX512-100	0.013400	0.674800	0.026300	0.233000
KM400	0.011000	0.662900	0.021600	0.202000

Table 9: Performance summary of chunking methods with different overlap settings. The metrics include Intersection over Union (IoU), Recall, Precision, and Precision@ Ω , each reported with their mean and standard deviation. All methods operate on 100-token chunks, enabling direct comparison of overlap effects.

Method	Chunk Size	Overlap Size	IoU	Recall	Precision@ Ω	Precision
FX100-0	100	0	0.064 \pm 0.049	0.678 \pm 0.423	0.344 \pm 0.138	0.065 \pm 0.049
FX100-20	100	20	0.067 \pm 0.049	0.704 \pm 0.426	0.287 \pm 0.097	0.068 \pm 0.049
FX100-40	100	40	0.069 \pm 0.049	0.727 \pm 0.418	0.251 \pm 0.078	0.069 \pm 0.049
FX100-60	100	60	0.069 \pm 0.050	0.725 \pm 0.422	0.224 \pm 0.066	0.069 \pm 0.050
FX100-80	100	80	0.067 \pm 0.051	0.706 \pm 0.431	0.204 \pm 0.060	0.068 \pm 0.051
RT100-0	100	0	0.090 \pm 0.067	0.711 \pm 0.408	0.365 \pm 0.149	0.091 \pm 0.067
RT100-20	100	20	0.090 \pm 0.066	0.709 \pm 0.412	0.357 \pm 0.142	0.091 \pm 0.067
RT100-40	100	40	0.088 \pm 0.065	0.714 \pm 0.416	0.332 \pm 0.136	0.089 \pm 0.066
RT100-60	100	60	0.086 \pm 0.062	0.724 \pm 0.413	0.311 \pm 0.132	0.086 \pm 0.062
RT100-80	100	80	0.084 \pm 0.061	0.724 \pm 0.414	0.304 \pm 0.131	0.085 \pm 0.062

Table 10: Precision and recall summary for chunking methods with varying overlap, sorted by F_2 score to emphasize recall-weighted performance. Colors in the associated visualization correspond F_2 scores.

Method	Precision_mean	Recall_mean	F_1	F_2
RT100-60	0.086200	0.724500	0.154100	0.563900
RT100-0	0.091200	0.711200	0.161600	0.563700
RT100-40	0.088900	0.714500	0.158200	0.562300
RT100-20	0.091100	0.708500	0.161400	0.562000
RT100-80	0.084500	0.723900	0.151400	0.560700
FX100-40	0.069300	0.727500	0.126500	0.532800
FX100-60	0.069100	0.724600	0.126200	0.530900
FX100-80	0.067600	0.706500	0.123500	0.518200
FX100-20	0.067600	0.704100	0.123400	0.517000
FX100-0	0.064700	0.678300	0.118200	0.497100